



UNIVERSITY OF LEEDS

This is a repository copy of *Permeability Prediction in Tight Carbonate Rocks using Capillary Pressure Measurements*.

White Rose Research Online URL for this paper:
<http://eprints.whiterose.ac.uk/90927/>

Version: Accepted Version

Article:

Rashid, F, Glover, PWJ, Lorinczi, P et al. (3 more authors) (2015) Permeability Prediction in Tight Carbonate Rocks using Capillary Pressure Measurements. *Marine and Petroleum Geology*, 68 (Part A). pp. 536-550. ISSN 0264-8172

<https://doi.org/10.1016/j.marpetgeo.2015.10.005>

© 2015. This manuscript version is made available under the CC-BY-NC-ND 4.0 license
<http://creativecommons.org/licenses/by-nc-nd/4.0/>

Reuse

Unless indicated otherwise, fulltext items are protected by copyright with all rights reserved. The copyright exception in section 29 of the Copyright, Designs and Patents Act 1988 allows the making of a single copy solely for the purpose of non-commercial research or private study within the limits of fair dealing. The publisher or other rights-holder may allow further reproduction and re-use of this version - refer to the White Rose Research Online record for this item. Where records identify the publisher as the copyright holder, users can verify any specific terms of use on the publisher's website.

Takedown

If you consider content in White Rose Research Online to be in breach of UK law, please notify us by emailing eprints@whiterose.ac.uk including the URL of the record and the reason for the withdrawal request.

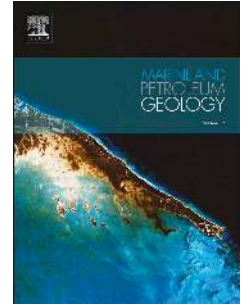


eprints@whiterose.ac.uk
<https://eprints.whiterose.ac.uk/>

Accepted Manuscript

Permeability Prediction in Tight Carbonate Rocks using Capillary Pressure Measurements

F. Rashid, P.W.J. Glover, P. Lorinczi, D. Hussein, R. Collier, J. Lawrence



PII: S0264-8172(15)30105-7

DOI: [10.1016/j.marpetgeo.2015.10.005](https://doi.org/10.1016/j.marpetgeo.2015.10.005)

Reference: JMPG 2364

To appear in: *Marine and Petroleum Geology*

Received Date: 2 July 2015

Revised Date: 28 September 2015

Accepted Date: 6 October 2015

Please cite this article as: Rashid, F., Glover, P.W.J., Lorinczi, P., Hussein, D., Collier, R., Lawrence, J, Permeability Prediction in Tight Carbonate Rocks using Capillary Pressure Measurements, *Marine and Petroleum Geology* (2015), doi: 10.1016/j.marpetgeo.2015.10.005.

This is a PDF file of an unedited manuscript that has been accepted for publication. As a service to our customers we are providing this early version of the manuscript. The manuscript will undergo copyediting, typesetting, and review of the resulting proof before it is published in its final form. Please note that during the production process errors may be discovered which could affect the content, and all legal disclaimers that apply to the journal pertain.

PERMEABILITY PREDICTION IN TIGHT CARBONATE ROCKS USING CAPILLARY PRESSURE MEASUREMENTS

Rashid, F.*, Glover, P.W.J., Lorinczi, P., Hussein, D., Collier, R., Lawrence, J.

School of Earth and Environment, University of Leeds, UK

* Email: eefnr@leeds.ac.uk, phone: +447445291315

Abstract. The prediction of permeability in tight carbonate reservoirs presents ever more of a challenge in the hydrocarbon industry today. It is the aim of this paper to ascertain which models have the capacity to predict permeability reliably in tight carbonates, and to develop a new one, if required. This paper presents (i) the results of laboratory Klinkenberg-corrected pulse decay measurements of carbonates with permeabilities in the range 65 nD to 0.7 mD, (ii) use of the data to assess the performance of 16 permeability prediction models, (iii) the development of an improved prediction model for tight carbonate rocks, and (iv) its validation using an independent data set. Initial measurements including porosity, permeability and mercury injection capillary pressure measurements (MICP) were carried out on a suite of samples of Kometan limestone from the Kurdistan region of Iraq. The prediction performance of sixteen different percolation-type and Poiseuille-type permeability prediction models were analysed with the measured data. Analysis of the eight best models is included in this paper and the analysis of the remainder is provided in supplementary material. Some of the models were developed especially for tight gas sands, while many were not. Critically, none were developed for tight gas carbonates. Predictably then, the best prediction was obtained from the generic model and the RGPZ models ($R^2 = 0.923, 0.920$ and 0.915 , respectively), with other models performing extremely badly. In an attempt to provide a better model for use with tight carbonates, we have developed a new model based on the RGPZ theoretical model by adding an empirical scaling parameter to account for the relationship between grain size and pore throat size in carbonates. The generic model, the new RGPZ Carbonate model and the two original RGPZ models have been tested against independent data from a suite of 42 samples of tight Solnhofen carbonates. All four models performed very creditably with the generic and the new RGPZ Carbonate models performing well ($R^2 = 0.840$ and 0.799 , respectively). It is clear from this study that the blind application of conventional permeability prediction techniques to carbonates, and particularly to tight carbonates, will lead to gross errors and that the development of new methods that are specific to tight carbonates is unavoidable.

35 KEYWORDS: capillary pressure, tight carbonates, permeability prediction, Kometan
36 limestone, Solnhofen limestone.

ACCEPTED MANUSCRIPT

38 Fluid permeability (Bernabé and Maineult, 2015) is one of the most important parameters in
39 reservoir characterisation and management. While measurable on core samples in the
40 laboratory, permeability is not available directly from downhole measurements. Since core
41 sample measurement is expensive and core samples only cover a small proportion of any
42 reservoir interval, other methods are required. Consequently, there exists a plethora of
43 empirical models which have been designed to calculate permeability from a wide range of
44 proxy measurements that often can be made downhole. We can classify these models into
45 different types.

46 One common type relates the absolute permeability to the grain size, pore size or
47 pore-throat size of the rock. These models can be considered to be percolation or
48 characteristic length scale models and relate the progress of the fluid through a porous
49 medium, which can be described by flow through an aperture with a single length scale.
50 Examples of this include the Kozeny-Carman (*e.g.*, Bernabé and Maineult, 2015, Schwartz *et al.*,
51 1986), Katz and Thompson (Katz and Thompson, 1986; 1987; Thompson *et al.*, 1987)
52 and RGPZ (Glover *et al.*, 2006) models. Walker and Glover (2010) considered the theoretical
53 basis for all of these models.

54 A second common model treats flow paths in the rock as a bundle of tubes, each of
55 which may have a different diameter. This is clearly a simplification of a porous medium, but
56 it is a different simplification than that used by the characteristic length scale models. Some
57 of these models include scaling coefficients, which enable this type of model to incorporate
58 different connectivities. Such an approach is then beginning to converge with the electrical
59 models represented by Archie's law (Archie, 1942), the modified Archie's law (Glover *et al.*,
60 2000), and the generalised Archie's law for n -phases (Glover, 2010). Examples of this
61 approach to permeability modelling include models by Swanson (1981), Wells and Amaefule
62 (1985), Winland (Kolodzie, 1980), Huet *et al.* (2005), Pittman (1992), Kamath (1992) and
63 Dastidar *et al.* (2007).

64 The main difference between the characteristic length scale (percolation) models and
65 the Poiseuille-type models is that the latter defines and calculates the flow paths in the model
66 exactly (as tubes) while the percolation models do not. Clearly, real rocks are rather more
67 variable than the Poiseuille-type models assume, and that variability is built into the
68 Poiseuille-type models by using empirical parameters that calibrate the model to a given
69 formation in a given reservoir. Consequently, each calibrated prediction model is specific to a
70 given reservoir, and errors would occur if the models were applied to another reservoir. This
71 introduces an important restriction to the Poiseuille-type models which reduces their

72 generality. However, in conventional reservoirs, the restriction is often balanced by the
73 advantage that the quality of prediction in a well-calibrated formation of a particular reservoir
74 is often extremely good.

75 By contrast, the characteristic length scale models build the variability of the porous
76 medium into the model, describing flow through the medium in terms of a characteristic
77 length scale. Often these length scales have a single value, such as the modal pore diameter in
78 a pore size distribution of the rock. This can work well if the rock has a well-defined and
79 narrow unimodal pore diameter distribution, but works less well if the rock has a wide or
80 multi-modal pore diameter distribution. Sometimes such models are implemented using a
81 distribution of characteristic length scales. The RGPZ model (Glover *et al.*, 2006), for
82 example, has been implemented in such a way that the overall permeability of a rock was
83 calculated from the geometric mean of the modal grain sizes weighted to account for the
84 distribution of those grain sizes within the rock (Glover *et al.*, 2006). Such an approach
85 makes the often unjustified assumption that the whole range of grain (pore or pore throat)
86 sizes that are being averaged contribute to the permeability of the sample.

87 In this work almost all the models were developed initially for conventional reservoirs
88 with permeabilities greater than 1 mD (Comisky *et al.*, 2007), although a few more recent
89 models, notably the Wells and Amaefule (1985) modification to the Swanson (1981) model
90 and the Huet *et al.* (2005) model were created specifically for tight gas sands with micro-
91 darcy permeabilities. None of the models tested in this paper have been developed for tight
92 gas carbonates with permeabilities in the nano-darcy to micro-darcy range. As far as we are
93 aware no models currently exist.

94 95 PERMEABILITY MODELS

96 The experimental data obtained in this study have been used to evaluate 16 permeability
97 models, which are listed in [Table 1](#). In this table a distinction is made between empirical
98 constants, which are constants that have been obtained empirically but are not usually
99 allowed to vary in the application of the model, and fitting parameters, which are parameters
100 that are commonly expected to be varied in the application the model in order to make the
101 model fit the data.

102 Eight of the sixteen models which were tested performed very badly when predicting
103 the permeability of tight carbonate rocks. The description of these models and a full analysis
104 of how well they performed has been excluded from this paper, but included as a file of
105 supplementary material which can be downloaded from the publisher's website. The eight
106 models which are included in the supplementary material encompass the Katz-Thompson

107 models using critical lengths and electrical length models (Katz and Thompson, 1986; 1987;
108 Thompson *et al.*, 1987), the Swanson model (Swanson, 1981), the Wells-Amaefule model
109 (Wells and Amaefule, 1981), the Kamath model (Kamath, 1992), the Huet *et al.* model (Huet
110 *et al.*, 2005), and the Berg Fontainebleau model (Berg, 2014). Three of these models are of
111 the percolation-type, and the remaining five are of the Poiseuille-type.

112 All of the models listed in Table 1 can be implemented using data obtained from
113 MICP measurements. The fundamental underlying equation which governs the MICP method
114 is what we now call the Washburn equation (Washburn, 1921), which relates the capillary
115 pressure P_c in a capillary tube of radius R , containing air and mercury in terms of the
116 interfacial tension σ and the wetting angle θ .

$$117 \quad P_c = \frac{2\sigma\cos\theta}{R} \quad (1)$$

118 The Washburn equation should properly be called the Bell-Cameron-Lucas-Washburn
119 equation because similar theoretical developments had been made three years before by
120 Lucas (1918) upon work on capillary pressures by Bell and Cameron in 1906 (Bell and
121 Cameron, 1906). For mercury and air, the interfacial tension $\sigma_{\text{Hg-air}} = 0.48$ N/m (480
122 dynes/cm) and the contact angle $\theta_{\text{Hg-air}} = 0^\circ$. In SI units, the use of R in meters gives the
123 capillary pressure in pascals. If imperial units are used, R in μm gives the capillary pressure
124 in psi.

125 Permeability is similar to electrical conductivity in that it can be thought of as being
126 partially controlled by the amount of pore space for hydraulic or fluid flow, and partially
127 controlled by how connected that pore space is (*e.g.*, Glover *et al.*, 2015). The assumption
128 that underlies all of the permeability models is that there is a particular length scale, or
129 distribution of length scales, that controls the permeability of the rock. In the case of the
130 percolation models, that length scale is given explicitly in the model either as a characteristic
131 length scale with an undefined physical expression, as the mean, modal or median grain
132 diameter, as the pore diameter calculated with the theta transformation (Glover and Walker,
133 2009), or as some measure of the pore throat size such as that obtained from MICP
134 measurements.

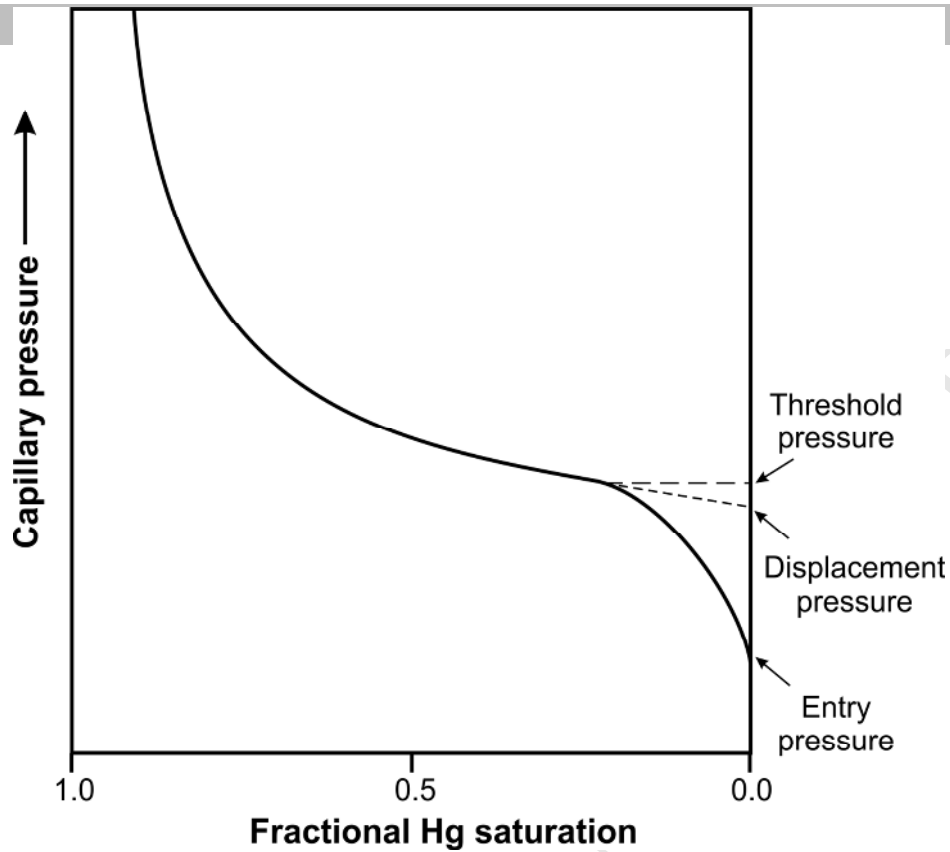
135 In the case of the Poiseuille models, the capillary pressure that corresponds to a given
136 characteristic length through Eq. (1) is used. One must, therefore, choose which point on the
137 capillary pressure curve to use in order to define the capillary pressure for permeability
138 modelling. It is this capillary pressure will be associated with a particular wetting fluid
139 saturation (air saturation for MICP measurements, and usually water saturation in the
140 reservoir).

141 The most commonly used points on the capillary pressure curve are the entry pressure
142 and threshold pressure (Figure 1). The entry pressure on the mercury-injection curve is the
143 point on the curve at which mercury initially enters the sample. This point is often indicative
144 of the largest pore throat size present in the sample and is usually associated with the largest
145 pores (Robinson, 1966). There is some uncertainty that such a measure really does represent
146 the largest pore throat size because (i) we are limited to the sample size and larger samples
147 may contain larger pore throats, and (ii) irregularities on the surface of the samples can mimic
148 large pores and give erroneous results when Eq. (1) is applied to them. Consequently, the
149 low-mercury saturation portion of the MICP curve may not be truly representative of the rock
150 (Bliefnick and Kaldi, 1996).

151 The threshold pressure is that at which the saturation of mercury increases
152 dramatically and corresponds graphically to an upward convex inflection point on the
153 mercury-injection curve. It represents the capillary pressure at which the greatest population
154 of pore sizes fill and for a unimodal pore throat size distribution indicates the pressure at
155 which the mercury can for the first time access the pores which represent the main fraction of
156 porosity in the rock. This point has been used profitably by Dewhurst *et al.* (2002) to quantify
157 the capability of mud-rocks to trap high pressure fluids. The threshold pressure point has
158 been experimentally determined by recording electrical resistance across a sample and
159 measuring the pressures at which continuity occurs (Katz and Thompson, 1986; 1987;
160 Thompson *et al.*, 1987).

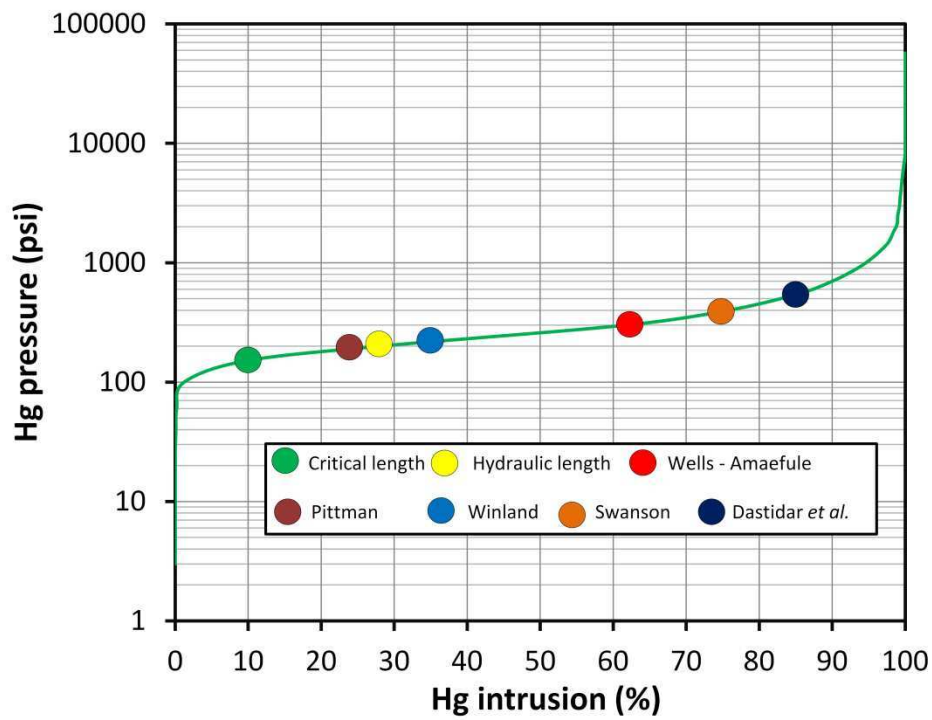
161 Pittman (1992) and Winland (Kolodzie, 1980; Comisky *et al.*, 2007; Gunter *et al.*,
162 2014) identified a mercury saturation percentile at which the reservoir threshold pressure can
163 be predicted to occur. Values of 3%, 5% and 10% (Schowalter, 1979) of the total mercury
164 saturation are considered by various researchers to predict the threshold pressure, although
165 such artificial restrictions are of no real utility since the threshold pressure depends upon the
166 rate of decrease of the tail of the pore throat size distribution which is sample-dependent.

167



168
169
170
171

Figure 1. Definition of the entry pressure, displacement pressure and threshold pressure of a MICP capillary pressure curve.



172
173
174

Figure 2. A typical capillary pressure curve for the MICP technique imposed upon which the length scales from the various models are used in this work.

175 **Table 1.** Fundamental properties and inputs of the sixteen models evaluated in this study.

Name	Parameters	No. of empirical constants	No. of fitting parameters	Reference
Percolation-based models				
Katz and Thompson – Critical length	<ul style="list-style-type: none"> • Critical length, L_c • Formation factor 	1	None	Katz and Thompson (1986; 1987), Thompson <i>et al.</i> (1987)
Katz and Thompson - Maximum electrical conductance length	<ul style="list-style-type: none"> • Maximum electrical conductance length, L_{Emax} • Critical length, L_c • Fraction of Hg-filled pore volume at L_{Emax}, S_{LEmax} • Porosity, ϕ 	1	None	Katz and Thompson (1986; 1987), Thompson <i>et al.</i> (1987)
Katz and Thompson - Maximum hydraulic length	<ul style="list-style-type: none"> • Maximum hydraulic length, L_{Hmax} • Critical length, L_c • Fraction of Hg-filled pore volume at L_{Hmax}, S_{LEmax} • Porosity, ϕ 	1	None	Katz and Thompson (1986; 1987), Thompson <i>et al.</i> (1987)
RGPZ theoretical approximate	<ul style="list-style-type: none"> • Characteristic grain diameter, d_{grain} • Cementation exponent, m • ‘a’-parameter • Porosity, ϕ 	1	None	Glover <i>et al.</i> (2006)
RGPZ theoretical exact	<ul style="list-style-type: none"> • Characteristic grain diameter, d_{grain} • Cementation exponent, m • ‘a’-parameter • Formation factor F, or porosity ϕ 	1	None	Glover <i>et al.</i> (2006)
RGPZ empirical carbonate	<ul style="list-style-type: none"> • Characteristic grain diameter, d_{grain} • Cementation exponent, m • ‘a’-parameter • Formation factor F, or porosity ϕ 	1	1	This work
Schwartz, Sen and Johnson (SSJ) generic form	<ul style="list-style-type: none"> • Characteristic pore size, Λ • Formation factor F 	1	1	Johnson <i>et al.</i> (1986); Johnson and Schwartz (1989); Johnson and Sen (1988); Schwartz <i>et al.</i> (1989)
Berg (Fontainebleau implementation)	<ul style="list-style-type: none"> • Porosity, ϕ 	4	4	Berg (2014) Equation (53)

Berg generic model	<ul style="list-style-type: none"> • Effective porosity, ϕ_s • Effective hydraulic tortuosity, τ_s • Constriction factor, C_s • Characteristic length L_h (equal to the radius of a capillary tube) 	1	None	Berg (2014) Equation (32)
Poiseuille-based models				
Swanson	<ul style="list-style-type: none"> • Apex value of Hg saturation to capillary pressure 	2	2	Swanson (1981)
Wells-Amaefule	<ul style="list-style-type: none"> • Apex value of Hg saturation to capillary pressure 	2	2	Wells and Amaefule (1985)
Kamath 'model'	<ul style="list-style-type: none"> • Apex value of Hg saturation to capillary pressure 	2	2	Kamath (1992)
Winland	<ul style="list-style-type: none"> • Length at which a mercury saturation is 35%, R_{35} • Porosity, ϕ 	3	3	Gunter et al. (2014)
Pittman	<ul style="list-style-type: none"> • Radius associated with the critical length L_c, R_{apex} • Porosity, ϕ 	3	3	Kolodzie (1980)
Dastidar <i>et al.</i>	<ul style="list-style-type: none"> • Weighted geometric mean of the pore size, R_{wgm} • Porosity, ϕ 	3	3	Dastidar <i>et al.</i> (2007)
Huet <i>et al.</i>	<ul style="list-style-type: none"> • Displacement pressure, P_d • Irreducible water saturation, S_{wi} • Porosity, ϕ • Brooks-Corey parameter, λ 	5	5	Huet <i>et al.</i> (2005)

176

177

178 **Table 1.** – cont.

179 **Percolation-based models**180 **Katz-Thompson [KT] models (Maximum Hydraulic Length)**

181 The Katz and Thompson models (Katz and Thompson, 1986; 1987; Thompson *et al.*, 1987)
 182 are based on percolation theory, and consider flow through a porous medium with random
 183 microstructure and connectivity. Flow is considered to be controlled by a length scale. There
 184 are three different length scales which are commonly used, each of which leads to a different
 185 permeability prediction model; the Critical Length (L_c), Maximum Hydraulic Length (L_{Hmax})
 186 and Maximum Electrical Conductance Length (L_{Emax}). The Maximum Hydraulic Length
 187 (L_{Hmax}) is described here, while the remaining two models are describe in the file of
 188 supplementary material.

189 The Maximum Hydraulic Length (L_{Hmax}) is defined as the effective pore throat
 190 diameter corresponding to the highest hydraulic conductance. The value of L_{Hmax} is the length
 191 corresponding to the capillary pressure at which the product of the mercury saturation and the
 192 pore throat diameter, $S_{Hg} \times d_{pt}$, is maximum. Katz and Thompson introduced a permeability
 193 model based on the length scale L_{Hmax} (Katz and Thompson, 1986; 1987; Thompson *et al.*,
 194 1987).

$$195 \quad k_{LH} = C_2 \left(\frac{L_{Hmax}^3}{L_c} \right) \phi S_{LHmax} \quad , \quad (2)$$

196 where the term L_{Hmax}^3/L_c provides the length-squared dimensions required for permeability,
 197 S_{LHmax} is the fraction of connected pore volume filled with mercury at L_{Hmax} , and the term
 198 ϕS_{LHmax} represents the fraction of the whole rock filled with mercury at L_{Hmax} . The parameter
 199 L_c is the critical length, which is defined as the critical pore diameter at which mercury forms
 200 a connected path through the sample, as shown in Figure 2. This occurs at the threshold
 201 pressure, which can be determined from the inflection point on a MICP curve. In this case the
 202 constant $C_2 = 1013/89$. The constant has empirical origins but is usually not varied to
 203 improve the fit or performance of the model.

204

205 **Schwartz, Sen and Johnson [SSJ] generic form**

206 A series of papers in the mid-80s (Johnson *et al.*, 1986; Johnson and Schwartz, 1989; Johnson
 207 and Sen, 1988; Schwartz *et al.*, 1989) led to the development of a characteristic length scale
 208 Λ for pores (Johnson *et al.*, 1986), and a new permeability model which used it. A
 209 generalised form of this equation may be written as

$$k_{SSJ} = \frac{\Lambda^2}{aF}, \quad (3)$$

where Λ is the Johnson *et al.* (1986) characteristic length scale of the pores, F is the formation factor and a is a constant that may be treated as a fitting parameter (Walker and Glover, 2010). This is an extremely simple model where the patency of the pores is expressed by the length scale and the connectedness of the pore flow paths is expressed by $1/F$.

It should be noted that the characteristic length scale of the pores is not some measure of the diameter or the radius of the pores in the usual sense; rather it is a measure of the effect of the pores on defining the transport properties of the pore network.

We cannot implement the SSJ model directly with our dataset because of the difficulty in finding an independent measurement of the characteristic length scale. Furthermore, calculation of the Λ parameter from our grain size, cementation exponent and formation factor would ensure that the SSJ model becomes formally the same as the RGPZ model. Instead, we have used Eq. (2) to generate a generic permeability model which shares some of the characteristics of both the SSJ and the RGPZ models. This equation may be written as

$$k_{GENERIC} = \frac{d_{grain}^2}{bF^3}, \quad (4)$$

where b is an empirically-determined parameter.

Walker and Glover (2010) took four of the most important models for predicting the permeability of porous media; the classical model of Kozeny and Carman [K-C] (*e.g.*, Bernabé, 1995), that of Sen, Schwartz and Johnson [SSJ] (Johnson *et al.*, 1986; Johnson and Sen, 1988; Schwartz *et al.*, 1989; Johnson and Schwartz, 1989), that of Katz and Thompson (Katz and Thompson, 1986; 1987; Thompson *et al.*, 1987) [KT], and the RGPZ model (Glover *et al.*, 2006). Each of these models is derived from a different physical approach. Walker and Glover (2010) rewrote them in a generic form which implied a characteristic scale length and scaling constant for each model. After testing the four models theoretically and against experimental data from 22 bead packs and 188 rock cores from a sand-shale sequence in the U.K. sector of the North Sea, they concluded that the Kozeny-Carman model did not perform well because it takes no account of the connectedness of the pore network and should no longer be used.

They discovered that the other three models all performed well when used with their respective length scales and scaling constants. Surprisingly, they found that the SSJ and KT models produce extremely similar results and their characteristic scale lengths and scaling

242 constants are almost identical even though they are derived using extremely different
 243 approaches: the SSJ model by weighting the Kozeny-Carman model using the local electrical
 244 field, and the KT model by using entry radii from fluid imbibition measurements.

245

246 RGPZ Model

247 Like the SSJ model, the RGPZ model (Glover *et al.*, 2006a) is also derived analytically and
 248 does not need calibration. The original equation is derived from the theoretical result that
 249 links the characteristic length scale Λ introduced by Johnston *et al.* (1986) to permeability
 250 through Eq. (2) and the approximate relationship between Λ and the electrical properties of
 251 the porous medium $\Lambda \approx d_{\text{grain}}/2mF$. The result is

$$252 \quad k_{RGPZ1} = \frac{d_{\text{grain}}^2 \phi^{3m}}{4am^2} = \frac{d_{\text{grain}}^2}{4am^2 F^3}, \quad (5)$$

253 where d_{grain} is some measure of the grain size which controls the flow properties of the
 254 porous medium, m is the cementation exponent (dimensionless), and ϕ is the porosity (as a
 255 fraction). It is important to note that the constant a is usually taken as 8/3 despite it being the
 256 same parameter that appears in Eq. (2). Consequently, it may be left to vary, and if so, the
 257 equation becomes empirical. It should be noted that this constant a is not the same as the
 258 Winsauer *et al.* modification to Archie's law (see Glover, 2015).

259 It has been pointed out that Eq. (5) relies on the formation factor being much greater
 260 than unity (*i.e.*, $F \gg 1$). While this is valid for clastic rocks without fractures, it may not be
 261 the case for rocks with low values of F such as those containing significant fractures. An
 262 exact form of the RGPZ equation, which is valid for all values of formation factor, can be
 263 obtained by replacing the approximation $\Lambda \approx d_{\text{grain}}/2mF$ with its exact form
 264 $\Lambda = d_{\text{grain}}/2m(F-1)$ (Revil and Cathles, 1999). This explains the failure of Eq. (5) for low F
 265 and corrects it, leading to

$$266 \quad k_{RGPZ2} = \frac{d_{\text{grain}}^2}{4am^2 F (F-1)^2}. \quad (6)$$

267 The definition of d_{grain} is critical to its implementation. For unimodal grain size distributions
 268 the use of the simple modal grain size gives permeabilities that can be overestimated. Glover
 269 *et al.* (2006b; 2006c) used Eq. (5) to compare the predictive powers of characteristic grain
 270 size obtained from the (i) modal value, (ii) weighted arithmetic mean, (iii) weighted harmonic
 271 mean, (iv) weighted geometric mean, and (iv) median values from grain size distributions

272 obtained from over 42 MICP measurements on glass bead packs, sands and reservoir rocks
 273 over a range from 100 mD to 100 D. The mean values were weighted by the grain size
 274 distribution across its entire range. The weighted geometric mean provided predicted
 275 permeabilities that were closest to those measured.

276 While the RGPZ has no variable coefficients and is theoretical in nature, unknown
 277 parameters such as, say, the cementation exponent, might be allowed to vary whereupon the
 278 model would become empirical. This study recognises that the RGPZ model was developed
 279 for clastic rocks and relies on their being a particular relationship between the grain size and
 280 the pore and pore throat sizes that seem to hold for clastic rocks but not for carbonates. This
 281 study has developed a new empirical permeability estimation method from the RGPZ model
 282 which is described later.

283

284 Berg (2014) Model

285 Recently, Berg (2014) has published a new model that attempts to use parameters that are
 286 both physically meaningful as well as being accessible experimentally. Berg's (2014) model
 287 can be written as

$$288 \quad k_{BERG2014} = \frac{\tau_s^2 L_h^2 \phi_s}{8C_s}, \quad (7)$$

289 where τ_s is the effective hydraulic tortuosity, L_h is the characteristic length relating to the
 290 flow process and becomes equal to the radius in a capillary tube special case solution of the
 291 equation, ϕ_s is the effective porosity, and C_s is called the constriction factor, and represents
 292 how flow paths become constricted in the direction of flow just as the fluid passes from pores
 293 into pore throats and out again.

294 The effective hydraulic tortuosity τ_s is the same as that used in the Kozeny-Carman
 295 formulations which is represented as the shortest flow length possible (*i.e.*, the length directly
 296 across the sample of rock) divided by the flow path length. This formulation of effective
 297 hydraulic tortuosity leads to smaller values when the flow is contorted rather than direct. In
 298 petrophysics we are more comfortable with the hydraulic tortuosity becoming larger if the
 299 flow is more contorted, so we will use that definition instead, rewriting the hydraulic
 300 tortuosity $\tau_h = 1/\tau_s$. Moreover, the electrical tortuosity is considered to be equal to the square
 301 of this hydraulic tortuosity $\tau_e = \tau_h^2$ and the definition of electrical tortuosity is $\tau_e = F\phi$, which
 302 allows Eq. (7) to be recast as

$$k_{BERG2014} = \frac{\phi^{1-m} L_h^2 (\phi - \phi_c)}{8C_s}, \quad (8)$$

where ϕ_c is the porosity that does not take part in fluid flow. We cannot determine ϕ_c and have therefore taken $\phi_c = 0$. We have also assumed that the characteristic length L_h can be represented by the Katz and Thompson hydraulic length L_{Hmax} used in Eq. (2). Taking all of these modifications into account the Berg (2014) model implemented in our study under the name of the 'Berg (2014) generic model' takes the form

$$k_{BERG2014} = \frac{L_{hmax}^2 \phi^{2-m}}{8C_s}, \quad (9)$$

where the constriction factor C_s is varied for the optimum fit, and hence the equation is used by use as an empirical relationship.

Poiseuille-based models

Winland Method

The models of Swanson, Wells and Amaefule and Kamath are all, in effect the same, differing only in the dataset upon which they have been calibrated. Winland, however, introduced a new approach, where the length scale was that at which a mercury saturation of 35% is attained, or R_{35} . The value of R_{35} is simply the radius calculated using the Washburn equation (Eq. (1)) from the capillary pressure corresponding to a mercury saturation of 0.35. Winland recognised that the permeability was related to both R_{35} and the porosity ϕ with an equation of the form

$$k_{Winland} = C_4 R_{35}^{a_2} \phi^{a_3}, \quad (10)$$

where C_4 , a_2 and a_3 are empirical variables, the permeability is calculated in mD and the R_{35} value is in μm .

The Winland model was originally described as a series of three unpublished reports for the Amoco Production Company, written between 1972 and 1976. These are consequently difficult to obtain and not referenced in this study. Instead we reference studies by Kolodzie (1980) and by Gunter *et al.* (2014), both of which discuss the Winland model in detail and the latter of which gives the full references of the original three reports.

333 Winland calibrated his equation using a dataset consisting of 82 samples (56
 334 sandstones and 26 carbonates) for which he had Klinkenberg-corrected permeabilities, and a
 335 further 240 samples for which only uncorrected air permeability data was available. The
 336 calibration gave $C_4 = 49.4$, $a_2 = 1.7$ and $a_3 = 1.47$. The range of the calibrating permeabilities
 337 is unknown but we do know, thanks to the research of Comisky *et al.* (2007) that they were
 338 made under ambient conditions.

339 The value of R_{35} is a rather crude way of defining the length scale that best
 340 characterises fluid flow in a complex medium. Nevertheless, other constant values, such as
 341 R_{40} , R_{50} have been suggested, but of those tested the R_{35} value, which corresponds to the
 342 largest pore throat sizes has been found to give the best result (Nelson, 1994; Kolodzie, 1980;
 343 Pittman, 1992).

344

345 Pittman Model

346 Pittman (1992) modified the Winland equation, using the length scale that corresponds to the
 347 threshold pressure instead of R_{35} . This length scale is the same as the critical length scale
 348 used by Katz and Thompson (Katz and Thompson, 1986; 1987; Thompson *et al.*, 1987), but
 349 is used by Pittman as a radius. The Pittman equation is

$$350 \quad k_{Pittman} = C_5 R_{ApeX}^{a_4} \phi^{a_5} . \quad (11)$$

351 Pittman calibrated this model using a set of 202 sandstone samples from 14 formations on
 352 which measured permeability, porosity, and mercury injection data had been obtained
 353 (Pittman, 1992) and obtained $C_5 = 32.3$, $a_4 = 1.185$, and $a_5 = 1.627$.

354 We have used our capillary pressure data to obtain a mean value for $R_{ApeX} =$
 355 0.135 ± 0.169 , corresponding to a mercury saturation of 35%. In other words, the points shown
 356 by the circles labelled Swanson and Winland in Figure 2 are very similar, and the two models
 357 are sampling the same fraction of the pore space.

358

359 **Model summary**

360 There is a striking difference between the percolation models and those based on the
 361 Poiseuille approach. The former need few empirical constants or sometimes none at all. The
 362 latter need two or even three such constants. Consequently, it might be expected that the
 363 Poiseuille-type models would provide better fits to data which are from similar formations,
 364 due to their specificity and the advantage of having more fitting parameters. However, they
 365 will perform much worse than the percolation models if they are used to predict the

366 permeability of rocks which do not share the characteristics of the rocks for which they were
367 calibrated.

368 Most of the models used in this paper were developed for use with clastic rocks, and
369 specifically for sandstone, with only a few being calibrated partially with carbonate samples.
370 Even the analytical RGPZ model was developed specifically for clastic rocks and has
371 traditionally not fared well in carbonates. The confining pressure of the measurements which
372 were used to calibrate the samples varied as well; from between 3000 to 4000 psi for the
373 model of Wells and Amaefule (1985) to only 800 psi or even ambient pressures in others
374 (e.g., Winland and Pittman). The permeability measurement approach also varied
375 significantly between all the models, including air permeabilities, steady-state and unsteady
376 state measurements, and pulse decay measurements. Some of these were corrected for
377 slippage, while others were not. Comisky *et al.* (2007) provide a useful table which compares
378 the experimental conditions of many of the permeability models listed above.

379 In other words, none of the methods summarised above were specifically derived for
380 tight carbonate rock samples (*i.e.*, for permeabilities less than 1.0 mD). This study uses
381 samples with permeabilities in the range 100 nD to 0.7 mD, and which exhibit no fractures or
382 microcracks.

383

384 MATERIALS AND MEASUREMENTS

385 Two suites of samples were used in this work.

386 The initial assessment of all 16 of the models used a suite of 125 core plugs from the
387 Kometan formation, originating from different outcrop locations or core material from a
388 number of different fields in the western segment of the Zagros basin in the northern part of
389 Iraq (Rashid *et al.*, 2015). For capillary measurements 25 plug samples were measured, of
390 which 3 failed to imbibe mercury because their pores were highly cemented. The effective
391 porosity of the samples ranged from 0.02 to 0.25, with a precision of ± 0.005 , while their
392 permeability ranged from 10 nD to 500 μ D.

393 The validation testing on the newly developed RGPZ Carbonate model, the generic
394 model and the two original RGPZ models used a suite of 42 core plugs from the Solnhofen
395 limestone from a quarry near Blumenburg. The samples show a range of effective porosity
396 from 0.11 to 0.14 with a mean of 0.044, measured with a precision of ± 0.005 , and which had
397 a permeability range from 11.5 nD to 176 μ D.

398 Prior to making any measurements, the cores were cleaned and dried using a Soxhlet
399 extraction process with low-temperature chloroform-methanol solutions according to the
400 American Petroleum Institute (API) recommended practices for core analysis. The samples
401 were then dried in a humidity-controlled environment. These cleaning and drying protocols
402 were initiated in order to reduce the effect of any damage or alteration of rock materials,
403 especially the clays that might enlarge pore spaces (Gant and Anderson, 1988).

404 The effective porosity of all the the Kometan samples was measured by helium
405 porosimetry using a Quantachrome stereopycnometer in the Wolfson Laboratory at the
406 University of Leeds, while the Solnhofen samples were measured using a high resolution
407 helium porosimeter that was designed and built by one of the authors of this paper and resides
408 in the Petrophysics Laboratory of the University of Leeds. The permeability of each sample
409 was measured using a helium pulse decay Klinkenberg-corrected permeability approach.
410 These measurements involve measuring the decay of gas pressure in an upstream reservoir as
411 the gas leaks through the sample. The measurements were carried out using a helium gas
412 pulse decay permeameter such as that in the Wolfson Laboratory of the University of Leeds
413 (Jones, 1997). At least four pulse decay tests were carried out for each rock sample, each with
414 different initial up-stream gas pressures in the range between 50 to 200 psi and downstream
415 pressures arranged such that the initial differential pressure was in the range of 5 to 40 psi.
416 All measurements of the Kometan limestone samples were made using a net confining
417 pressure of 800 psi, while all the Solnhofen samples were made at a net confining pressure of
418 725 psi, and at a temperature of 25° C in each case. The net confining pressure is very
419 important for tight rocks as permeability can vary greatly as a function of this parameter. All
420 permeability measurements were corrected for slippage effects as these can also be very
421 significant in tight rocks.

422 Considerable efforts were made to optimise the quality of these small porosity and
423 permeability measurements, including the preparation of high quality cylindrical core plugs.

424 The capillary pressure curve was measured using a high pressure mercury injection
425 capillary pressure technique, which involves injecting mercury into an evacuated core sample
426 in a stepwise fashion (Melrose, 1990). The volume of mercury injected at each pressure is a
427 measure of the non-wetting (*i.e.*, mercury) saturation. This method is relatively fast, usually
428 requiring only hours to complete each measurement. In addition, MICP techniques are
429 capable of applying injection pressures as great as 60,000 psi, which provides coverage of
430 almost the entire range of water saturation and capillary pressure for tight carbonate rock
431 samples, as well as for higher porosity and permeability reservoir quality rocks (Torsaeter

432 and Abtahi, 2000). The MICP technique has some disadvantages, which include the use of
433 mercury as a proxy for the reservoir non-wetting phase (usually a hydrocarbon) and air used
434 as the wetting phase, when in a reservoir it is usually water. Mercury-air capillary pressure
435 measurements made in this way require conversion to give the value they would have in a
436 reservoir using reservoir fluids and at reservoir pressure and temperature. This correction is
437 carried out using contact angle and surface tension measurements on the mercury-air-rock
438 system and on the reservoir fluid-rock system at reservoir conditions. Although the MICP
439 technique ensures that the sample cannot be used for further tests and must be disposed of
440 safely, the technique can be used on samples with irregular shapes, including drill cuttings
441 (Jennings, 1987). In this study tests were carried out using a MicroMeritics 33 Porotech IV
442 apparatus (Webb, 2001). The non-wetting phase was injected using 62 pressure steps which
443 were distributed logarithmically. The selection of penetrometer size is derived from the
444 combination of the sample volume and porosity (Giesche, 2006). Acceptable capillary
445 pressure results can be achieved when at least 20% of the penetrometer stem volume is
446 displaced into the rock sample. Tight rock samples with low porosities require larger sample
447 volumes for any selected penetrometer size. In this work penetrometers with stem volumes
448 between 0.392 cm^3 to 1.131 cm^3 were used. A mercury-air-rock contact angle of 140 degrees
449 and the mercury-air surface tension of 480 dynes/cm (0.48 N/m) (Webb, 2001) was used
450 throughout this work.

451 The MICP measurements were either used directly in modelling, which was usually
452 the case for the Poiseuille-based models, or were used to calculate a modal pore throat size
453 which could then be used to calculate a modal pore size or a modal grain size using
454 techniques of Glover and Déry (2010) and Glover and Walker (2009), respectively, for
455 subsequent use in modelling with the percolation-based models.

456 Some of the models also require the formation factor and cementation exponent to be
457 known. These were obtained by measuring the electrical properties of each of the samples
458 after they have been saturated with an aqueous solution. Full saturation of such tight samples
459 is a very difficult thing to carry out. In our case it involved a combination of evacuation and
460 saturation under a vacuum followed by pressurisation. The formation factor is best obtained
461 by making a number of electrical measurements while the rock is saturated with pore fluids
462 of different salinity. However, because the rocks are so tight we chose in all cases to calculate
463 the formation factor from the electrical resistivity measured on the rock at 1 kHz while it was
464 saturated with a single salinity of pore fluid together with the resistivity of that pore fluid.
465 The method for doing this is straightforward and can be found in the review by Glover (2015)

466 together with methods for measuring the resistivity of the pore fluid itself. A simple equation
467 links the cementation exponent to the formation factor and porosity, and hence the
468 cementation exponent for each sample can also be calculated simply, as also set out in Glover
469 (2015).

470 POROSITY & PERMEABILITY

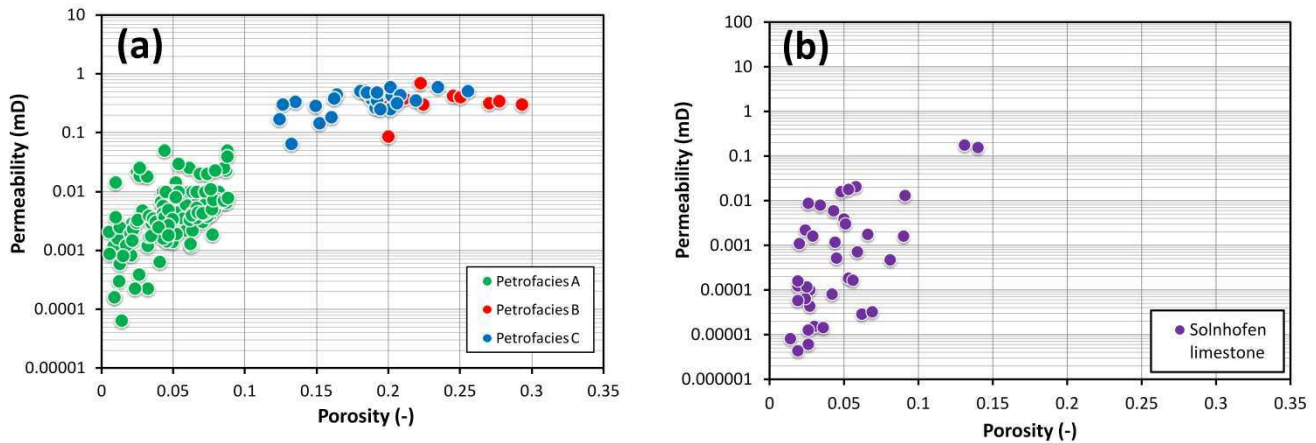
471 Figure 3 shows a poroperm cross-plot of all the measured Kometan limestone data, some of
472 which was used in the initial modelling, as well as the Solnhofen data that was used as an
473 independent data set for testing purposes.

474 Figure 3a classifies the samples according to a petrofacies classification that is
475 discussed in Rashid *et al.* (2015). In this figure Petrofacies A is a compact
476 wackstone/packstone which has lost almost all of its primary porosity due to cementation,
477 containing nanometer-sized intercrystalline pores, and which contains occasional
478 microfractures and stylolites and consequently has a very low porosity and permeability.
479 Petrofacies B is a dissolved wackstone/packstone that contains moldic and vuggy pores, and
480 Petrofacies C is a carbonate mudstone that has undergone dissolution and possibly some
481 dolomitisation. Figure 4 shows typical scanning electronmicrographs for each petrofacies.

482 The petrophysical behavior of the samples is controlled by a complex pore geometry
483 system, governed by throat size, pore size and diagenetic alteration. The poroperm diagram
484 shows each petrofacies distinctly. Petrofacies A comprises the first group and is well
485 separated from the other two petrofacies in the bottom, left-hand corner of the poroperm
486 diagram due to its low porosity and permeability, varying between 10 nD and 10 μ D (green
487 symbols). This type of rock has porosities in the range 0.01 to 0.08 and a wide range of
488 permeabilities. The large spread of permeabilities reflects the large range of pore connectivity
489 present within this fabric, while the positive trend shows that any small increase in porosity
490 provides an enhancement of the connectivity of the pore network sufficient to increase the
491 permeability of the sample. There is some overlap between Petrofacies B and C (the blue and
492 red symbols in Figure 3, respectively), but both show significantly larger porosities and
493 correspondingly larger permeabilities. The relatively flat poroperm trend of Petrofacies C
494 shows that increasing porosity (in the range 0.18 to 0.28) is not significantly enhancing
495 permeability in the sample, which is in the range 0.08 to 4 mD. This agrees well with our
496 observation that moulds and vugs tend to be relatively unconnected to the pore network.
497 Petrofacies B has a well constrained porosity range, from about 0.08 to about 0.25, and an
498 equally well constrained permeability range. Overall there is a positive poroperm trend for

499 Petrofacies B, showing that higher porosities caused by dissolution also lead to higher
 500 permeabilities (Rashid *et al.*, 2015).

501



502

503

504 **Figure 3.** (a) Poroperm cross-plot of the three facies of Kometan limestone used in this
 505 paper for initial testing of the 16 permeability models, and (b) Poroperm cross-plot of the
 506 Solnhofen limestone data that was used as an independent data set for testing four of the
 507 better-performing models including the newly developed RGPZ Carbonate model.

508

509 Figure 5 shows a plot of the capillary pressure type-curves, demonstrating the full
 510 range of the capillary pressure curves within the Kometan limestone dataset. The entry
 511 pressure and displacement pressure of each group varies. A high entry pressure was recorded
 512 for all samples, reflecting the tightness of all of the samples.

513 From the examination of thin section and SEM results of the representative samples,
 514 we see a trend of decreasing pore size with decreasing pore throat size implying increasing
 515 entry capillary pressure values and decreasing permeability. However, there is no similar
 516 relationship between the pore size and grain size. The moldic pores have greater diameter
 517 because they are derived from the dissolution of foraminifer chambers. Consequently, there is
 518 no relationship between the size of these large moldic pores and the modal grain size of the
 519 rock. This observation allows us to predict that the models which were developed for clastic
 520 rocks and in which there is an implicit assumption that the pore and pore throat size are
 521 related to the grain size, such as the RGPZ model, may not perform well in carbonates in
 522 general and specifically in tight carbonates.

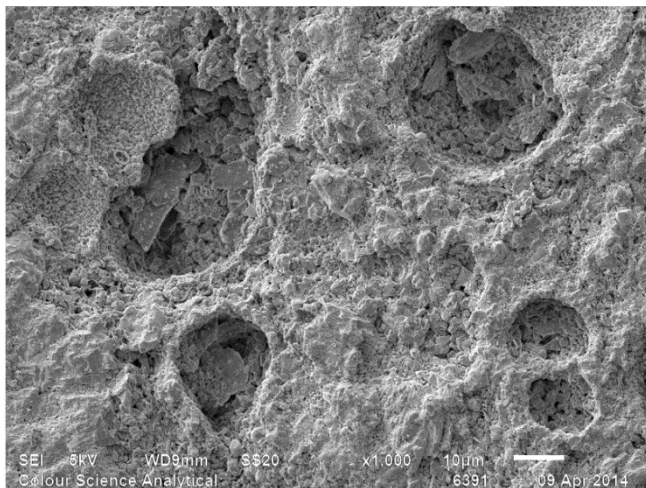
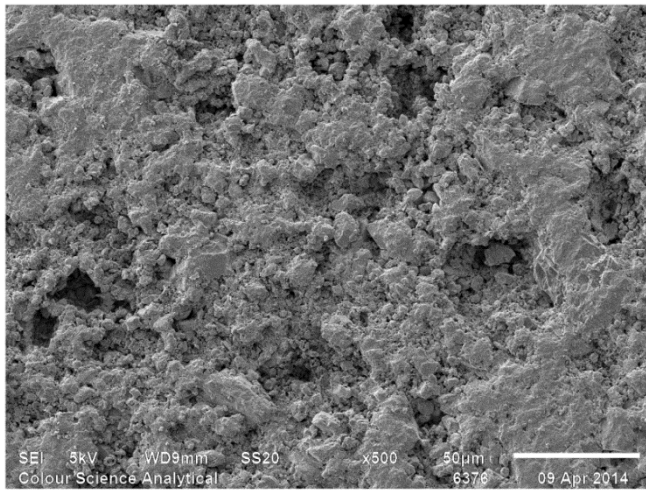
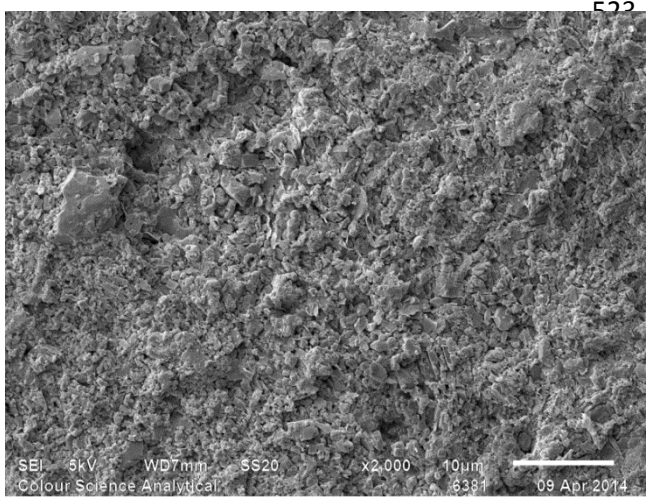
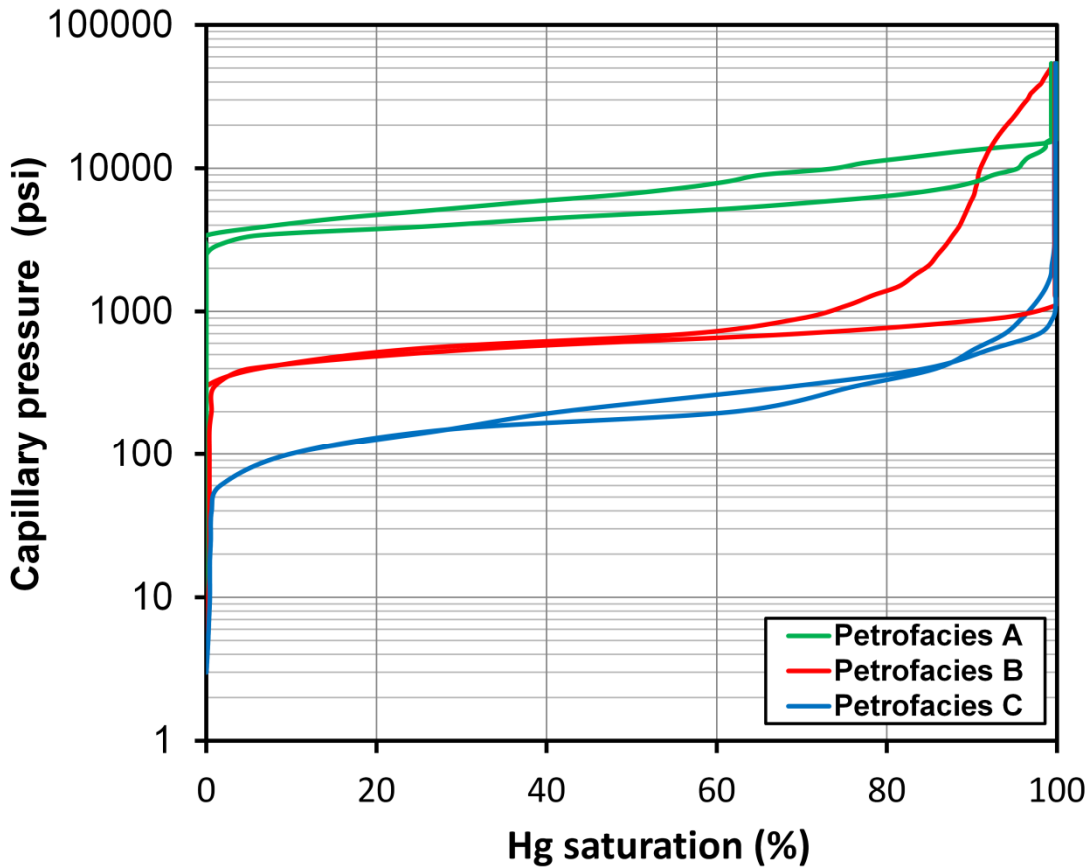


Figure 3b shows the poroperm diagram for the Solnhofen limestone data, exhibiting a surprisingly large range of permeabilities for the zero to 0.1 porosity range. Many of these samples show a trend which overlaps that of Kometan limestone Petrofacies A.

Figure 4. Scanning electronmicrographs of the three facies of rocks studied in this work; Petrofacies A, upper; Petrofacies B, middle and Petrofacies C, lower.



550

551 **Figure 5.** Mercury injection capillary pressure curves for typical samples from each of the
 552 three petrofacies used in this work.

553

554 A NEW MODEL FOR TIGHT CARBONATES

555 During our initial testing of the models with the Kometan limestone samples it became clear
 556 that a new and better model was needed for tight carbonate rocks, and we decided to try to
 557 develop one. Subsequently, this model was also tested with the Kometan limestone dataset,
 558 and then, as will be shown later in this paper, applied to another independent dataset of
 559 Solnhofen limestone.

560 In developing the new model we decided to take the theoretical RGPZ model as a
 561 starting point for a number of reasons. First, one of the authors had many years understanding
 562 the model having been one of those developing it initially. Second, the model has a
 563 theoretical pedigree so that any modifications made to ensure that it performs better in
 564 carbonate rocks can be understood as simple perturbations to an already well-understood
 565 relationship, rather than a complex interaction with previous empirical developments. Third,
 566 the model had shown itself to already be fairly good at predicting the permeability of

567 carbonate rocks, being ranked third and fourth of the sixteen models were initially tested.
568 Finally, it was thought that the reasons behind the failure of the RGPZ model in tight
569 carbonates was known, and might be corrected for by modification.

570 In clastic rocks there is a relationship between pore size and grain size. This arises
571 from the fact that clastic rocks are composed of eroded grains which are usually sub-
572 spherical. When the clastic rock contains some grains which have a plate-like shape, such as
573 micas, they are usually not present in a fraction sufficiently large enough to cause gross
574 changes to the microstructure of the pores. In this scenario, increasing the size of grains
575 clearly increases the size of the pores, and one might think that the pore throats would
576 increase in size as well. This idea has led to a mathematical transformation between pore size
577 and grain size for clastic rocks to be produced (Glover and Walker, 2009), where the
578 coefficient proportionality between the pore size and grain size is called the ‘theta’
579 transformation, and depends upon the cementation exponent m , the formation factor F , and
580 the constant $a=8/3$. The relationship in clastic rocks between pore size and grain size holds
581 good providing there has not been significant diagenesis that alters the amount and
582 distribution of pore space within the rock.

583 In carbonates, however, it is common that there has been a large amount diagenesis,
584 which has altered the distribution of pore spaces within the rock by successive episodes of
585 dissolution, precipitation and recrystallisation. In this case, there is no simple or unique
586 relationship between grain size and pore size. Indeed, grains may be very large, complex and
587 interlocking with each other, while the pore spaces between them have small volumes and are
588 linked by tortuous pore throats. Increasing grain sizes are now not necessarily related to
589 increased pore sizes, and if they are the relationship will be very different to that for clastic
590 rocks. However, analysis of the results in this paper for the two conventional RGPZ models
591 shows them to do fairly well, but tend to overestimate the measured permeability. We
592 therefore hypothesise that we may get a much better prediction by scaling the theta
593 transformation, associating increases in grain size with smaller increases and pore size. The
594 RGPZ model uses a modal grain size as a length scale. However, it is a pore or pore throat
595 length scale that will ultimately control fluid flow. The implication is that we will still be able
596 to use an RGPZ-style model, with a grain size input parameter, for carbonate rocks but the
597 scaling factor will then take account of the fact that the input grain size is not necessarily
598 associated with pore size as large as it would be if the rock was a clastic rock.

599 The use of a grain size as an input parameter ensures that the RGPZ model is easy to
600 apply with widely available core data, but it implies that the RGPZ model incorporates a

601 relationship that converts, or interprets the grain size in a way which can influence a
 602 predicted permeability as a pore or pore throat scale would. The question, therefore is
 603 whether this internal relationship, which has been proven to work well for clastic rocks
 604 (Glover *et al.*, 2006) is also applicable to carbonates.

605 Consequently, we have produced a new model by taking the RGPZ exact model and
 606 scaling the formation factor by an arbitrary factor η which is greater than unity, leading to a
 607 larger formation factor than would be expected from the porosity and cementation exponents
 608 of the samples. This process recognises that the connectedness of the pores involved in fluid
 609 flow is less in carbonates than in a clastic rock of the same grain size. This process converts
 610 the theoretical RGPZ model into an empirical model because the η -factor is now an
 611 empirically-determined coefficient that can be viewed as a fitting parameter. The resulting
 612 equation is

$$613 \quad k_{RGPZCarbonate} = \frac{d_{grain}^2}{4am^2\eta F(\eta F - 1)^2} \approx \frac{d_{grain}^2}{4am^2\eta^3 F^3} \quad (12)$$

614
 615 The approximation is valid in the limit $F \gg 1$, and applies in this study because the formation
 616 factors in tight carbonate rocks are generally very high, varying between 23 and 2565 with a
 617 mean value of 314. The approximation will also be valid for most reservoir rocks, even those
 618 with relatively high porosities.

619 Since the variation of η for individual samples would result in the trivial result of a
 620 perfect prediction, we have shown the result for $\eta=1.73$ in Figure 6f. This value was chosen
 621 as the center of the range in which the fitting statistics were optimised. It is worth noting that
 622 in the limit $F \gg 1$, the implementation of $\eta=1.73$ is the equivalent of having a formation
 623 factor or tortuosity that is 73% higher, a cementation exponent 9.53% higher (for $F=314$), or
 624 a grain, pore or pore throat size that is 43.9% of that assumed by the standard RGPZ model,
 625 accounting for the observation that diagenetic processes in carbonates have reduced the
 626 effective pore size with respect to the effective grain size.

627

628 PERMEABILITY PREDICTION

629 In total we tested 16 models and all are included in Table 1 for completeness. This number
 630 includes the model that we have developed in this paper and describe later in the paper. Eight
 631 of the models performed particularly badly when applied to tight carbonates. Consequently,
 632 they are not reported in detail in this paper. However, their full description, concordance plots

633 and discussion is presented in a file of supplementary material available from the publishers
634 website. These models are those of the Katz-Thompson using critical lengths and electrical
635 length (Katz and Thompson, 1986; 1987; Thompson *et al.*, 1987), the Swanson model
636 (Swanson, 1981), the Wells-Amaefule model (Wells and Amaefule, 1981), the Kamath
637 model (Kamath, 1992), the Huet *et al.* model (Huet *et al.*, 2005), and the Berg Fontainebleau
638 model (Berg, 2014).

639 The remaining eight models, which are described further in this paper are the Katz-
640 Thompson model using hydraulic length models (Katz and Thompson, 1986; 1987;
641 Thompson *et al.*, 1987), the Berg generic model (Berg, 2014), the Winland (Comisky *et al.*,
642 2007; Gunter *et al.*, 2014) and Pittman models (Pittman, 1992), the exact and approximate
643 forms of the original RGPZ model, a generic form of the RGPZ/SSJ model (Glover *et al.*,
644 2006), and finally the model developed in this paper, which is a modification of the RGPZ
645 model for carbonate rocks, and which we have called the RGPZ Carbonate model.

646 Figure 6 shows how well each of the models predicts the measured permeability for
647 each sample of the Kometan limestone dataset. Each part of Figure 6 contains a 1:1 line that
648 indicates a perfect prediction as well as high and low bounds representing a variance of ± 2.5
649 (i.e., upper and lower bounds representing 2.5 times greater or less than a perfect prediction,
650 respectively). A simple judgement concerning the goodness of prediction is that the
651 prediction falls between the variance ± 2.5 limits.

652 Percolation-type models tend to perform better than Poiseuille-type models, with only
653 two of the Poiseuille-based models performing well enough to be discussed in the main
654 paper. These are the models of Pittman and of Winland. Of the percolation models that did
655 not perform well, two only failed marginally – the critical length and electrical length models
656 of Katz and Thompson (Katz and Thompson, 1986; 1987; Thompson *et al.*, 1987), while the
657 Berg (2014) model specific to Fontainebleau sandstone, unsurprisingly failed in carbonates.

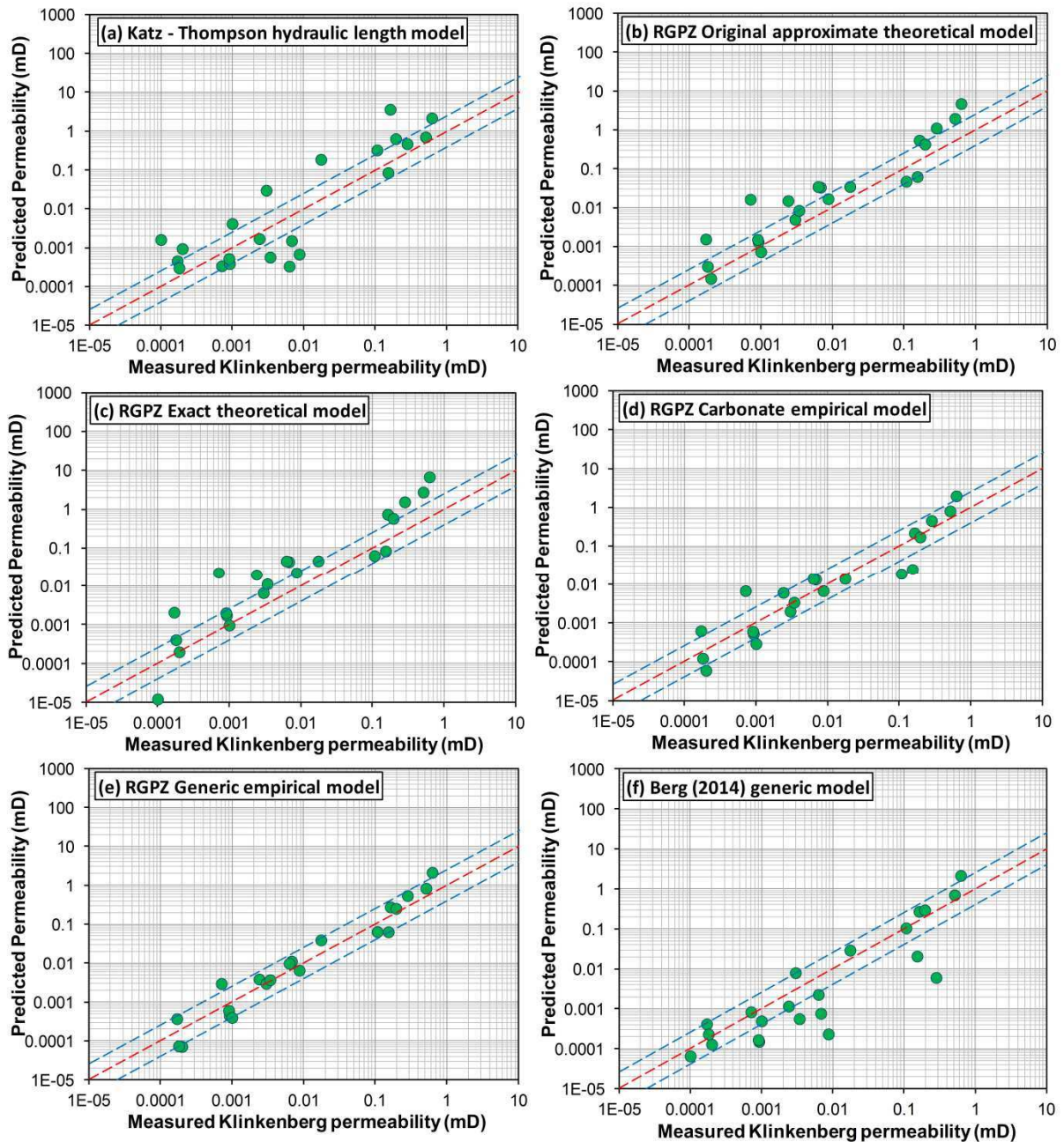
658 The best performance was that of the Generic model and occurred for a value of
659 $88 < b < 100$. The new RGPZ empirical carbonate model also performed well with $1.7 < \eta < 1.76$.
660 Both the exact and approximate forms of the standard RGPZ model (Glover *et al.*, 2006) also
661 performed creditably, but produced a tendency to overestimate the permeability occasionally
662 by as much as an order of magnitude. Since the formation factors of tight carbonate rocks are
663 so high we might expect the two forms of the model to produce very similar results. This is
664 borne out by Figure 6. Calculation of the mean ratio of the permeability predicted using the
665 approximate form of the model to that using the exact form gives 0.979 ± 0.0023 , showing

666 how close the predictions are, and that the approximate form produces slightly lower
667 predicted permeabilities.

668 Of the Katz and Thompson (Katz and Thompson, 1986; 1987; Thompson *et al.*, 1987)
669 models, the hydraulic conductivity model produced the best match with the measured
670 Klinkenberg-corrected permeability for these tight carbonates. However, while the general
671 trend of the permeability predicted with this technique matches the measured permeability
672 well, there is a large scatter and individual samples may have permeabilities up to an order of
673 magnitude larger or smaller than the real permeability.

674 The two best Poiseuille-based models were those of Pittman (Pittman, 1992;
675 Kolodzie, 1980; Comisky *et al.*, 2007; Gunter *et al.*, 2014) and of Winland (Gunter *et al.*,
676 2014), with the majority of the predictions falling within the ± 2.5 variance criterion. The
677 Winland model is one of the simplest that we have, and it is instructive that it was calibrated
678 using Klinkenberg-corrected permeabilities. Nevertheless, the success of the Winland model
679 for our data and possibly other tight carbonates might rely on a happy coincidence that its use
680 of a mercury saturation of 35% upon which to base the length scale is close to the value for
681 rocks which share the texture (porosity and connectedness) of tight carbonates.

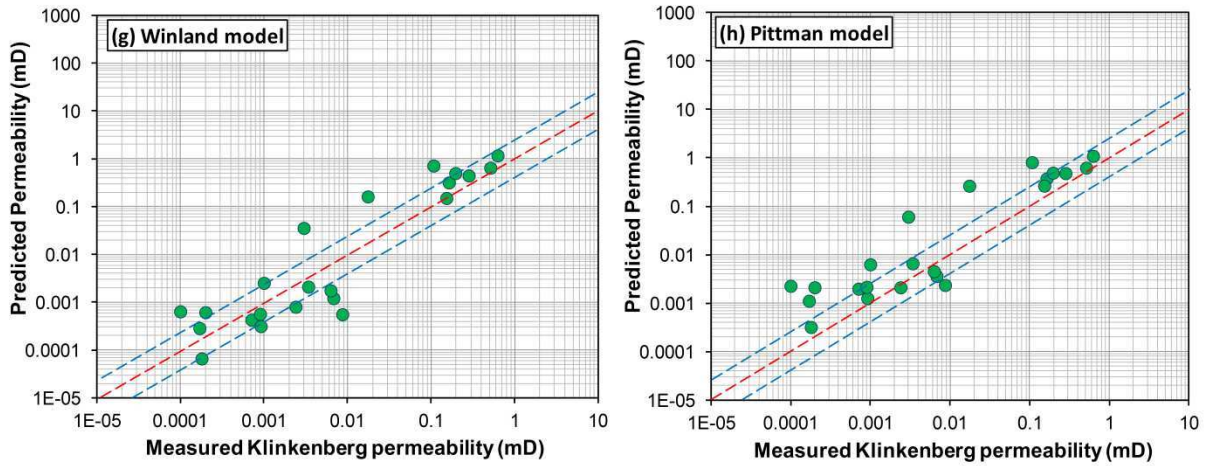
682 The Pittman model (Pittman, 1992) is a modification of the Winland model using a
683 length scale corresponding to the threshold pressure instead of R_{35} . For the rocks studied in
684 this work the Pittman model provided predictions of permeability that were a slight
685 improvement on those from the Winland model, over estimating permeability by about half
686 an order of magnitude. The use of the threshold pressure instead of R_{35} led, in our study to an
687 increase in the predicted permeability by a factor that was greater than unity in all but 3
688 samples and had an arithmetic mean of 2.62 ± 1.31 using standard deviation to express the
689 uncertainty. It is clear from a comparison of these two models that, at least for the tight
690 carbonate rocks in our data, the length scale which controls the permeability of the rock
691 sample is closer to that associated with the threshold pressure than that associated with the
692 R_{35} point, and is larger than the length scale associated with the R_{35} point.



693

694 **Figure 6.** The performance of the 8 best models in predicting the permeability of a suite of
 695 Kometan limestone samples, together with a 1:1 perfect agreement and variance lines set at
 696 ± 2.5 . For (e) $b=94$, (d) $\eta=1.73$, and (f) $C_s=3.4$.

697



698

699

Figure 6. –cont.

700

701

702

703

704

705

We have quantified the performance of the prediction using three measures. These are: (i) the percentage of samples with predictions falling within ± 2.5 times the measured permeability, to which we give the symbol ξ , (ii) the root mean squared residual of log values (RMSLR), and (iii) the Pearson product-moment correlation coefficient (PPMCC). The RMSLR is calculated using the equation

706

$$RMSLR = \sqrt{\frac{1}{n} \sum_{i=1}^n [\log(K_{L,i}) - \log(K_{est,i})]^2}, \quad (13)$$

707

708

where n is the sample population size, $K_{est,i}$ is the value of the predicted permeability, and $K_{L,i}$ is the measured Klinkenberg-corrected permeability.

709

710

711

712

713

714

Table 2 shows the prediction performance statistics for all 16 models, for completeness. This table also gives a rank value for each test and an overall rank which is the rank of the unweighted sum of the three individual ranks. On this basis the best two models are the generic percolation model and the new RGPZ Carbonate model, and the worst two are the Berg (2014) Fontainebleau model which is a percolation-based model calibrated for this sandstone, and the Huet *et al.* model which is a Poiseuille-based model.

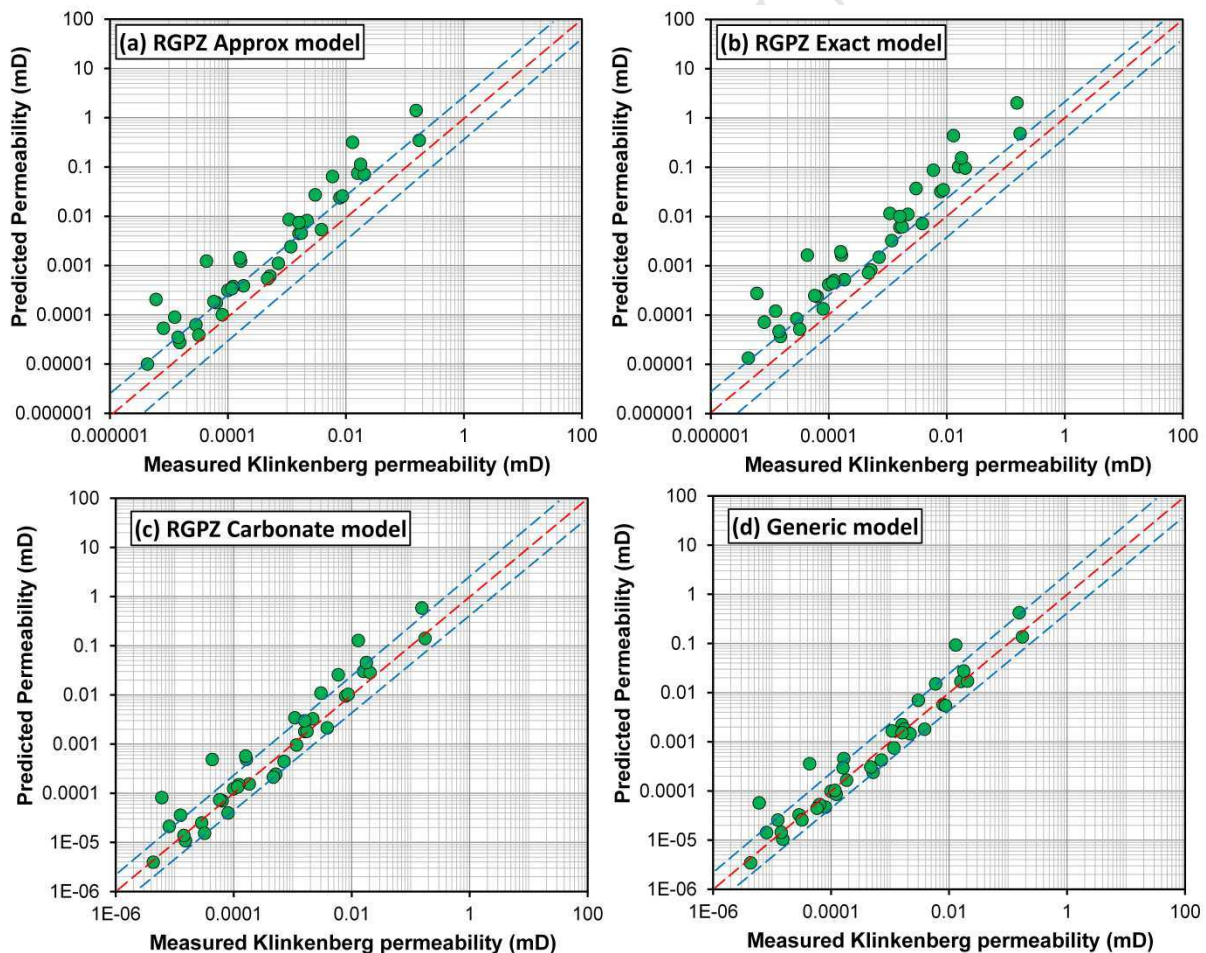
715 **Table 2.** Quantitative measures of permeability prediction effectiveness.

ξ (%)	Rank on ξ	RMSLR	Rank on RMSLR	PPMCC	Rank on PPMCC	Overall rank	Permeability model	Type
81.818	1	0.402	1	0.923	1	1	Generic model (Eq. (4))	Percolation
68.182	2	0.576	3	0.917	4	2	RGPZ empirical carbonate model	Percolation
54.545	5=	0.609	4	0.920	2	3	RGPZ approximate theoretical model	Percolation
54.545	5=	0.618	5	0.915	5	4=	RGPZ exact theoretical model	Percolation
59.091	3=	0.654	6	0.903	6	4=	Winland model	Poiseuille
40.909	7	0.576	2	0.872	7	6	Pittman model	Poiseuille
59.091	3=	0.696	7	0.858	10	7	Berg (2014) generic model	Percolation
31.818	9	0.969	9	0.918	3	8	Katz and Thompson-Electrical length model	Percolation
36.364	8	0.724	8	0.575	14	9	Katz and Thompson-Hydraulic length model	Percolation
27.273	10	1.066	10	0.683	12	10	Katz and Thompson-Critical Length model	Percolation
4.545	13=	1.358	11	0.827	11	11	Wells and Amaefule model	Poiseuille
13.636	11=	1.605	12	0.613	13	12	Dastidar <i>et al.</i> model	Poiseuille
0.000	15=	1.976	13	0.866	9	13	Kamath 'model'	Poiseuille
0.000	15=	2.204	15	0.868	8	14	Swanson model	Poiseuille
13.636	11=	2.003	14	0.485	15	15	Berg (2014) Fontainebleau model	Percolation
4.545	13=	2.277	16	0.174	16	16	Huet <i>et al.</i> model	Poiseuille

ξ : Percentage of samples whose prediction is within a factor of ± 2.5 of the real permeability.
RMSLR: Root mean squared log residuals, see Eq. (13).
PPMCC: Pearson product-moment correlation coefficient

716 TESTING THE NEW MODEL

717 Although the new RGPZ Carbonate model performed very well when predicting the
 718 permeability of the Kometan limestone samples, we felt that it was necessary to validate the
 719 new model by testing it against an independently obtained dataset. Consequently, we used a
 720 dataset of 42 samples of Solnhofen limestone, which have already been described in an
 721 earlier section of this paper. We did not restrict the permeability prediction to solely the new
 722 RGPZ Carbonate model, but also carried out prediction with the two original RGPZ models
 723 and the generic model. This was done so that the testing on the new RGPZ Carbonate model
 724 could be viewed in the context of other well-performing models. It was particularly
 725 interesting to us to see whether the modifications made to the existing RGPZ models made
 726 any significant improvements when used in predicting the permeability of tight carbonates.
 727



728

729 **Figure 7.** The performance of (a) the RGPZ approximate model, (b) the RGPZ exact model,
 730 (c) the new RGPZ carbonate model and (d) the generic model, in predicting the permeability
 731 of a suite of 42 Solnhofen limestone samples, together with a 1:1 perfect agreement and
 732 variance lines set at ± 2.5 . For (c) $\eta=1.5$, and (d) $b=100$.

733

734 Figure 7 shows the results of the modelling. All four models performed creditably, but
735 once again the two original RGPZ models have a tendency to overestimate the permeability
736 in a subset of the samples. The Pearson product-moment correlation coefficient (PPMCC)
737 was 0.801 and 0.797, respectively. Both the new RGPZ carbonate model (PPMCC=0.799)
738 and the generic model (PPMCC=0.840) produced very good fits considering how small these
739 permeabilities are.

740 It should be noted that Figure 7 was produced by setting $\eta=1.5$, and $b=100$ for the
741 new RGPZ carbonate model and the generic model, respectively. These values could be
742 considered as fitting parameters, and varied to find the best fit for a particular rock type. We
743 have not attempt to do so, but doing so might improve the fit marginally in each case. The
744 value of these parameters depends upon how the grain size and pore throat sizes are
745 interrelated. Consequently, there is the potential for finding a physical control behind these
746 parameters in tight carbonates which would then allow them to be calculated independently.

747

748 DISCUSSION

749 All of the models considered in this study use MICP measurements to provide a length scale
750 from which a permeability can be calculated. In most cases, it is a single length scale that is
751 defined on the assumption that the pore throat size at a given mercury saturation is special in
752 that it represents the length scale that either controls or represents the permeability of the
753 rock. Different definitions are used by different models. However, given the great complexity
754 of rocks, it is unlikely that a length scale based on a single length measurement is likely to be
755 effective in describing the permeability of a range of different rocks.

756 Another approach calculates a single effective length scale from a weighted (usually
757 geometric) mean of all pore or pore throat sizes. The RGPZ method has been applied in this
758 approach fairly effectively (Glover *et al.*, 2006a; 2006b; 2006c), and the method is used in
759 the method of Dastidar *et al.* (2007).

760 Whatever the method used to obtain the single, hopefully representative, value that is
761 to be used as a length scale, the fact remains that it is a single value, and much of
762 effectiveness of the prediction process depends upon it. In choosing a model, we are choosing
763 which definition of the length scale we think will produce the most accurate permeability
764 predictions.

765 Fourteen of the 16 models studied in this work contain coefficients that must be
766 obtained empirically. These models need to be calibrated against a typical dataset where the
767 permeability has been measured and is accurately known. It is important that these calibration
768 measurements are made on the same type of materials and under the same conditions as the
769 model will be applied. Consequently, the calibration for a tight carbonate should be carried
770 out on tight carbonates using Klinkenberg-corrected pulse decay gas pressure measurements
771 at a well-defined overburden pressure. These criteria were not fulfilled for any of the
772 empirical models tested. There were few calibration datasets that contained any carbonates
773 and there were no tight carbonates, while some calibration sets included tight clastic rocks.
774 Some calibration sets used gas permeabilities with undefined flow pressures, while others
775 used steady-state liquid permeabilities and a third group used unsteady-state pulse decay
776 measurements. In some of these measurements the flow pressures were not controlled, and
777 only a few calibration datasets had Klinkenberg-corrected their calibration data. Some
778 measurements were made at low equivalent overburden pressures, while others used a
779 consistent high value. In summary, the quality of the prediction depends upon the quality of
780 the calibration, and that was often very poor.

781 We associate the relative success of the Winland method with the fact that it was
782 calibrated with a suite of cores that contained a significant number of carbonates, that the
783 pulse decay permeability measurement was used and that all measurements were
784 Klinkenberg-corrected. In all of these respects the Winland model approaches the conditions
785 under which we measured our rock samples. It might be inferred, therefore, that the Winland
786 model's use of a pore throat radius being filled when 35% of mercury saturation is attained is
787 particularly valid for these tight carbonates. The slightly better predictions provided by the
788 Pittman approach might suggest that the threshold pressure is an even better characteristic
789 point upon which to base the pore throat scale length. The Katz-Thompson hydraulic length
790 characteristic method also provides acceptable permeability predictions for our tight
791 carbonate samples which implies that the highest hydraulic conductance of the Katz-
792 Thompson model is close to the R_{35} point for tight carbonate rocks. A cross-plot of the
793 permeability predicted using the Katz and Thompson model as a function of that predicted
794 with the Winland model shows a remarkable correlation with only a few samples not falling
795 on a 1:1 straight line.

796 The Dastidar *et al.* (2007) model is one of the more complex models tested. It applies
797 the weighted geometric mean approach that was used by Glover *et al.* (2006a; 2006b; 2006c)
798 with the RGPZ model. The concept in using this approach is that the permeability of the rock

799 is defined not by a single length scale, but by an ensemble of length scales from the very
800 largest to the very smallest according to how many pores of each size compose the rock. The
801 geometric mean is chosen because it represents the permeability of a random ensemble of
802 sub-volumes of the sample that have individual permeabilities. Consequently, using a
803 weighted geometric mean of the MICP pore throat sizes before applying the permeability
804 prediction equation is equivalent to calculating the permeability with the permeability
805 prediction equation for each pore throat size and then taking a weighted geometric mean of
806 the resulting permeabilities, providing the permeability prediction equation is linear. All of
807 the models investigated in this study fulfil this criterion.

808 Despite its complexity, the Dastidar *et al.* (2007) model did not perform well for tight
809 carbonates. This may be due partly to their use of sandstones, but the previously mentioned
810 averaging process may also be invalid in this application. It is interesting to note that the
811 weighted geometric mean length scale (R_{wgm}) that we calculated for each sample was always
812 significantly larger than R_{25} and R_{35} , which was the cause of the general overestimation of
813 permeability resulting from this model. This would then imply that the weighted geometric
814 averaging procedure was taking too much account of the largest pores in the rock. The
815 corollary is that the largest pores in tight carbonates do not contribute much to the overall
816 permeability of the rock, an observation that has been made previously by Rashid *et al.*
817 (2015). The implication is that the weighted geometric mean approach might work in tight
818 carbonates providing that the calculation was not done over the entire range of MICP data,
819 but ignores the largest pores. One might also make an argument for restricting the range of
820 the weighted geometric mean calculation to exclude the very smallest pores on the basis that
821 these small pores would have a capillary pressure too high for the pores to transmit fluids
822 under normal reservoir pressures.

823 Many of the more successful models that have been the subject of this paper use
824 electrical data in the form of the formation factor or the cementation exponent, or both. It is
825 interesting to ask the question whether these electrical data are accurate when made on tight
826 rocks. It is notoriously difficult to fully saturate a tight carbonate. The formation factor
827 measured on such a saturated tight carbonate will be that which relates to the pore network
828 that is saturated with pore fluid. If the entire pore network is not saturated with pore fluid the
829 measured formation factor will be higher than if it was completely saturated. It will be that
830 higher formation factor which will be used to predict permeability, and consequently the
831 predicted permeability will be lower than if the rock was fully saturated. The extent of this
832 problem is difficult to gauge, and it would be a useful subject to further study. One would

833 expect that there would be a systematic difference between the Klinkenberg-corrected
834 permeability measured on a tight carbonate rock with a gas like helium, which can percolate
835 through all of the pores no matter how small and the permeability measured with a liquid, and
836 one would expect the permeability predicted using a method that require the use of the
837 measured formation factor to also be smaller than the measured Klinkenberg-corrected gas
838 permeability.

839

840 CONCLUSIONS

841 There are many models that purport to be able to estimate or predict the permeability of rocks
842 for the purposes of reservoir characterisation, almost all of which were developed for high
843 porosity and high permeability conventional clastic reservoirs. However, the current need is
844 for models that will work in unconventional tight reservoirs which are often in carbonate
845 lithologies, with low permeabilities, and have a degree of heterogeneity and anisotropy.

846 A common approach to permeability prediction uses data from mercury injection
847 capillary pressure (MICP) measurements. We have taken sixteen MICP-based models and
848 have tested how well they predict the permeability of a suite of tight carbonate core plugs
849 from the Kometan formation in the north-east of Iraq. These include 7 existing percolation-
850 based models, 8 Poiseuille-based models, and a percolation-based model that we have
851 developed in this paper. We have included the full analysis of 8 of the models which show
852 the best performance in this paper, and have made available the full analysis of the remaining
853 eight in supplementary material which may be downloaded from the publisher's website.

854 All the permeability measurements presented in this paper were made by pulse decay
855 permeametry. All measurements were Klinkenberg-corrected, and were carried out at a fixed
856 overburden pressure of 800 psi for the Kometan limestone samples and 725 psi for the
857 Solnhofen limestone samples. Mercury injection capillary pressure measurements were made
858 on all samples. The permeability prediction methods often require supporting data such as
859 formation factor, and these were made independently.

860 It was expected that many of the models that were developed for high permeability
861 clastic rocks would fail badly when asked to predict the permeability of tight carbonates, and
862 this was indeed the case. In general percolation-based models performed much better than
863 Poiseuille-based models, though the Pittman model and Winland model performed creditably.
864 The best performing model was the simplest, being a generic model of the percolation type
865 upon which both the SSJ and RGPZ models are based, and both versions of the RGPZ model

866 also performed well. Consequently, we are led to the conclusions that (i) the blind application
867 of conventional permeability prediction techniques to carbonates, and particularly to tight
868 carbonates, will lead to gross errors, and (ii) the development of new methods that are
869 specific to tight carbonates is unavoidable.

870 There are many reasons why the predictions for many of the models are so bad. They
871 include:

- 872 1. The models were designed for high porosity and permeability clastic rocks.
- 873 2. The models were calibrated only in the high porosity, high permeability range.
- 874 3. The models were calibrated with data that had not been Klinkenberg-corrected.
- 875 4. The models were calibrated with data made at zero or uncontrolled overburden
876 pressures.
- 877 5. The models were calibrated using a mixture of permeability measurement approaches
878 including methods that are irrelevant to tight rocks.
- 879 6. Carbonate rocks do not have the same relationships between grain size, pore size and
880 pore throat size as clastic rocks due to their pore microstructure and particularly their
881 pore connectedness being affected by post-depositional diagenesis.

882
883 Consequently, we developed a new model based on the RGPZ theoretical model by
884 adding an empirical parameter to account for the relationship between grain size and pore
885 throat size in carbonates in an attempt to provide a better model for use with tight carbonates.
886 We have tested this new RGPZ Carbonate model, together with the generic model, and the
887 two original RGPZ models have been tested against laboratory permeability measurements
888 made on a suite of 42 samples of tight Solnhofen carbonate. In this dataset, the permeability
889 was measured using a Klinkenberg-corrected pulse decay technique at an overburden
890 pressure of 725 psi. These samples were also subjected to helium porosimetry, and electrical
891 measurements in order to obtain the formation factor and cementation exponents. Finally,
892 each sample was submitted to Mercury Injection Capillary Pressure measurements to obtain a
893 modal pore throat size, and modal pore sizes and grain sizes were calculated, providing a full
894 set of measurements required to predict the permeability using the four chosen methods.

895 All of the four models tested at this stage performed very creditably with the new RGPZ
896 Carbonate performing second best ($PPMCC = 0.799$). Perhaps surprisingly the best two
897 models, the generic model and the new RGPZ Carbonate model are also simplest, containing
898 only one empirical coefficient. It should also be remarked that the two original forms of the
899 RGPZ model, which also performed creditably, despite being strictly valid only for clastic

900 rocks, were the only theoretical models in the 16 tested, and consequently did not need to be
901 calibrated with experimental data.

902 In the light of needing to develop new and different ways to predict the permeability
903 of tight carbonates, it has been suggested that one approach might be to use multi-
904 dimensional imaging techniques such as CT scanning. If this were to be successful for tight
905 carbonates it would not only imply the use of extremely high-resolution CT scanning such as
906 that provided by NanoXCT imagers, but also the development of software that was capable
907 of reliably modelling fluid flow in the resulting digital pore microstructure model.

908

909 ACKNOWLEDGEMENTS

910 It is greatly appreciated that this study was funded by the Ministry of Higher Education of the
911 Iraqi Kurdistan Region government as a part of the Human Capacity Development
912 Programme (HCDP). We also express our gratitude to the Ministry of Natural Resources of
913 Kurdistan Region and the Ministry of Oil of the Iraqi government for providing some project
914 data. Thanks are also due to Dr. Carlos Grattoni of the Wolfson Laboratory at Leeds
915 University for his help in the laboratory.

916

917 REFERENCES

918

919 ARCHIE, G.E. 1942. The electrical resistivity log as an aid in determining some reservoir
920 characteristics: Transactions of the American Institute of Mechanical Engineers, 146, 54–67.

921

922 BELL, J.M. & CAMERON, F.K. 1906. The flow of liquids through capillary spaces. J. Phys. Chem. 10:
923 658–674. doi:10.1021/j150080a005.

924

925 BERG, C.F. 2014. Permeability Description by Characteristic Length, Tortuosity, Constriction and
926 Porosity. Transport in Porous Media, 103(3), pp. 381-400.

927

928 BERNABÉ, Y. 1995. The transport properties of networks of cracks and pores. Journal of Geophysical
929 Research, 100(B3), pp. 4231-4241.

930

- 931 BERNABÉ, Y. & MAINEULT, A. 2015. Physics of Porous Media: Fluid Flow Through Porous Media. In:
932 Gerald Schubert (editor-in-chief) Treatise on Geophysics, 2nd edition, Vol 11. Oxford:
933 Elsevier;. p. 19-41.
934
- 935 BLIEFNICK, D.M. & KALDI, J.G. 1996. Pore geometry: control on reservoir properties, Walker Creek
936 field, Columbia and Lafayette Counties, Arkansas. *AAPG Bulletin*, 80, 1027-1044.
937
- 938 COMISKY, J.T., NEWSHAM, K., RUSHING, J.A. & BLASINGAME, T.A. 2007. A Comparative Study of
939 Capillary-Pressure-Based Empirical Models for Estimating Absolute Permeability in Tight Gas
940 Sands. Society of Petroleum Engineers.
941
- 942 DASTIDAR, R., SONDERGELD, C.H. & RAI, C.S. 2007. An Improved Empirical Permeability Estimator
943 From Mercury Injection For Tight Clastic Rocks.
944
- 945 DEWHURST, D.N., JONES, R.J. & RAVEN, M.D. 2002. Microstructural and petrophysical
946 characterization of Muderong Shale: application to top seal risking. *Petroleum Geoscience* 8,
947 371–383.
948
- 949 GANT, P.L. & ANDERSON, W. G. 1988. Core Cleaning for Restoration of Native Wettability.
950
- 951 GIESCHE, H. 2006. Mercury Porosimetry: A general (practical) overview. Particle & particle systems
952 characterization. 23, 9-19.
953
- 954 GLOVER, P.W.J. 2009. What is the cementation exponent? A new interpretation. *Leading Edge*
955 (Tulsa, OK), 28(1), pp. 82-85.
956
- 957 GLOVER, P.W.J. 2010. A generalized Archie's law for n phases. *Geophysics*, 75(6), pp. E247-E265.
958
- 959 GLOVER, P.W.J. 2015. Geophysical Properties of the Near Surface Earth: Electrical Properties. In:
960 Gerald Schubert (editor-in-chief) Treatise on Geophysics, 2nd edition, Vol 11. Oxford:
961 Elsevier; 2015. p. 89-137.
962
- 963 GLOVER, P.W.J., HOLE, M.J. & POUS, J. 2000. A modified Archie's law for two conducting phases.
964 *Earth and Planetary Science Letters*, 180(3-4), pp. 369-383.

- 965
966 GLOVER, P.W.J., ZADJALI, I.I. & FREW, K.A. 2006a. Permeability prediction from MICP and NMR data
967 using an electrokinetic approach. *Geophysics*, 71(4), pp. F49-F60.
968
- 969 GLOVER, P.W.J., ZADJALI, I. & FREW, K. 2006b. Permeability prediction from MICP and NMR data
970 using an electro-kinetic approach, Poster, EGU 2006, EGU06-A-01566, Vienna, 2-7 April
971 2006.
972
- 973 GLOVER, P.W.J., ZADJALI, I. & FREW, K. 2006c. A new equation for permeability prediction derived
974 from electro-kinetic theory., Oral, GAC-MAC-SEG-SGA 2006, Abstract No. 758, Montréal, 14-
975 17 May 2006.
976
- 977 GLOVER, P.W.J. & WALKER, E. 2009. Grain-size to effective pore-size transformation derived from
978 electro-kinetic theory. *GEOPHYSICS*, 74, 17-29.
979
- 980 GUEGUEN, Y. & PALCIAUSAKAS, V. 1994. *Intoruction to the physics of rocks*, NJ, Princeton University
981 press
982
- 983 GUNTER, G.W., SPAIN, D.R., VIRO, E.J., THOMAS, J.B., POTTER, G., & WILLIAMS, J. 2014. Winland
984 Pore Throat Prediction Method - A Proper Retrospect: New Examples From Carbonates and
985 Complex Systems. Society of Petrophysicists and Well-Log Analysts SPWLA-2014-KKK, SPWLA
986 55th Annual Logging Symposium, 18-22 May, Abu Dhabi, United Arab Emirates.
987
- 988 HUET, C.C., RUSHING, J.A., NEWSHAM, K.E. & BLASINGAME, T.A. 2005. A Modified Purcell/Burdine
989 Model for Estimating Absolute Permeability from Mercury-Injection Capillary Pressure Data.
990 International Petroleum Technology Conference, Doha, Qatar, Nov. 21-23, Paper IPTC
991 10994.
992
- 993 JENNINGS, J.B. 1987. Capillary Pressure Techniques: Application to Exploration and Development
994 Geology. *AAPG Bulletin*, 71, 1196-1209.
995
- 996 JOHNSON, D.L., KOPLIK, J. & SCHWARTZ, L.M. 1986. New pore-size parameter characterizing
997 transport in porous media: *Physical Review Letters*, 57, no.20, 25642567,
998 doi:10.1103/PhysRevLett.57.2564

- 999
- 1000 JOHNSON, D.L., & SCHWARTZ, L.M. 1989. Unified theory of geometrical effects in transport
1001 properties of porous media: Presented at 30th Annual Symposium, Society of Petrophysicists
1002 and Well Log Analysts paper E, 1–25.
- 1003 JOHNSON, D.L., & SEN, P.N. 1988. Dependence of the conductivity of a porous medium on
1004 electrolyte conductivity: *Physical Review B: Condensed Matter and Materials Physics*, 37, no.
1005 7, 3502–3510, doi: 10.1103/Phys.RevB.37.3502.
- 1006 JONES, S.C. 1997. A Technique for Faster Pulse-Decay Permeability Measurements in Tight Rocks.
1007
- 1008 KAMATH, J. 1992. Evaluation of Accuracy of Estimating Air Permeability From Mercury-Injection
1009 Data.
1010
- 1011 KATZ, A.J. & THOMPSON, A.H. 1986. Quantitative prediction of permeability in porous rock. *Physical*
1012 *Review B*, 34, 8179-8181.
- 1013
- 1014 KATZ, A.J. & THOMPSON, A.H. 1987a. Prediction of rock electrical conductivity from mercury
1015 injection measurements. *Journal of Geophysical Research: Solid Earth*, 92, 599-607.
1016
- 1017 KOLODZIE, S., JR. 1980. Analysis Of Pore Throat Size And Use Of The Waxman-Smits Equation To
1018 Determine Ooip In Spindle Field, Colorado. Society of Petroleum Engineers.
1019
- 1020 LUCAS, R. 1918. Ueber das Zeitgesetz des Kapillaren Aufstiegs von Flüssigkeiten. *Kolloid Z.* 23: 15.
1021 doi:10.1007/bf01461107.
1022
- 1023 MELROSE, J.C. 1990. Valid Capillary Pressure Data at Low Wetting-Phase Saturations (includes
1024 associated papers 21480 and 21618).
1025
- 1026 NELSON, P.H. 1994. Permeability-porosity Relationships In Sedimentary Rocks.
1027
- 1028 PITTMAN, E.D. 1992. Relationship of porosity and permeability to various parameters derived from
1029 mercury injection-capillary pressure curves for sandstone. *AAPG Bulletin*, 76, 191-198.
1030

- 1031 RASHID, F., GLOVER, P.W.J., LORINCZI, P., COLLIER, R., & LAWRENCE, J. 2015. Porosity and
1032 permeability of tight carbonate reservoir rocks in the north of Iraq, *Journal of Petroleum*
1033 *Science and Engineering*, 133, 147–161, <http://dx.doi.org/10.1016/j.petrol.2015.05.009>
1034
- 1035 REVIL, A. and, CATHLES, L.M. 1999. Permeability of shaly sands: *Water Resources Research*, 35, 651–
1036 662.
1037
- 1038 ROBINSON, R.B. 1966. Classification of reservoir rocks by surface texture. *AAPG Bulletin* 50, 547-559.
1039
- 1040 SCHOWALTER, T.T. 1979. Mechanics of secondary hydrocarbon migration and entrapment. *AAPG*
1041 *Bulletin*, 63.
1042
- 1043 SCHWARTZ, L.M., SEN, P.N. & JOHNSON, D.L. 1989, Influence of rough surfaces on electrolytic
1044 conduction in porous media: *Physical Review B: Condensed Matter and Materials Physics*,
1045 40, no. 4, 2450–2458, doi: 10.1103/PhysRevB.40.2450
1046
- 1047 SWANSON, B. F. 1981. A Simple Correlation Between Permeabilities and Mercury Capillary
1048 Pressures.
1049
- 1050 THOMEER, J.H.M. 1960. Introduction of a pore geometrical factor defined by the capillary pressure
1051 curve. *Pet. Tech*, 73-77.
1052
- 1053 THOMPSON, A.H., KATZ, A.J., & RASCHKE, R.A. 1987. Estimation of Absolute Permeability from
1054 Capillary Pressure Measurements. Paper SPE 16794 presented at the 1987 SPE Annual
1055 Technical Conference and Exhibition, Dallas, TX, Sept. 27-30.
1056
- 1057 TORSÆTER, O. & ABTAHI, M. 2000. *Experimental reservoir engineering laboratory workbook*,
1058 Department of petroleum engineering and applied geophysics, Norwegian University of
1059 Science and Technology, Trondheim, Norway, Lab rep.
1060
- 1061 WALKER, E. & GLOVER, P.W.J. 2010. Characteristic pore size, permeability and the electrokinetic
1062 coupling coefficient transition frequency in porous media, *Geophysics*, 75(6), E235-E246,
1063 2010. [pdf] , doi: 10.1190/1.3506561
1064

- 1065 WASHBURN, E.W. 1921. The Dynamics of Capillary Flow. *Physical Review*, 17, 273-283.
1066
- 1067 WEBB, P.A. 2001. An Introduction to the physical characterization of materials by mercury intrusion
1068 porosimetry with emphasis on reduction and presentation of experimental data. Norcross,
1069 Georgia.
1070
- 1071 WELLS, J.D. & AMAEFULE, J.O. 1985. Capillary Pressure and Permeability Relationships in Tight Gas
1072 Sands. Society of Petroleum Engineers.
1073
1074

Highlights

- The Kometan Formation classified as tight carbonate reservoir.
- 16 existing models of permeability prediction have been applied.
- The generic percolation model and the new RGPZ empirical are the two best percolation model of permeability prediction.
- The Winland and Pittman methods are the two Poiseuille-based models that are provided a good result.

PERMEABILITY PREDICTION IN TIGHT CARBONATE ROCKS USING CAPILLARY PRESSURE MEASUREMENTS: SUPPLEMENTARY MATERIAL

Rashid, F.*, Glover, P.W.J., Lorinczi, P., Hussein, D., Collier, R.

School of Earth and Environment, University of Leeds, UK

* Email: eefnr@leeds.ac.uk, phone: +447445291315

This document contains information about 9 permeability prediction models of the 16 which were tested during the work described in Rashid et al. “Permeability Prediction in Tight Carbonate Rocks using Capillary Pressure Measurements”, but which were found to be sufficiently ineffective when applied to tight carbonate rocks to not warrant their inclusion in the main paper.

The supplementary information is structured in two parts. The first describes each of the models. The second describes a comparison of the use of these models with independently measured pulse-decay gas permeability measurements. This data may be merged with the data in the main paper to provide a comparison of the effectiveness of all 16 models included in the study.

PERMEABILITY MODEL DESCRIPTIONS

This section describes the models which were found to be relatively ineffective in predicting the permeability of tight carbonate rock samples.

Percolation-based models

Katz-Thompson models

The Katz and Thompson model is in fact three models, two of which are too ineffective in carbonates to be described in the main paper and hence are described here. Since all three models are related, all three models will be described in this section.

The Katz and Thompson models are based on percolation theory, and consider flow through a porous medium with random microstructure and connectivity. Flow is considered to be controlled by a length scale, one for each version of the model, and each is defined differently.

The first model is the Critical Length (L_c) model, where the critical length is defined as the critical pore diameter at which mercury forms a connected path through the sample, as shown in [Figure 2](#) of the main paper. This occurs at the threshold pressure, which can be determined from the inflection point on a MICP curve. This model was shown to be ineffective in carbonates and is not included in the main paper.

The second model uses a characteristic length called the Maximum Hydraulic Length (L_{Hmax}). This is defined as the effective pore throat diameter corresponding to the highest hydraulic conductance. The value of L_{Hmax} is the length corresponding to the capillary pressure at which the product of the mercury saturation and the pore throat diameter, $S_{Hg} \times d_{pt}$, is maximum. This model was shown to perform reasonably in carbonates and is included in the main paper.

The third model uses a characteristic length called the Maximum Electrical Conductance Length (L_{Emax}), which is the effective pore throat diameter where ionic conductance is maximized. It is evaluated as the length corresponding to the capillary pressure at which the product of the mercury saturation and the pore throat diameter cubed, $S_{Hg} \times d_{pt}^3$ is maximum. This model was also shown to be ineffective in carbonates and is not included in the main paper.

One might think that L_{Hmax} and L_{Emax} would be the same if the porosity and pore connectivity remained the same. However, there exist pore spaces within the rock that are patent to fluid flow but closed to electrical flow due to ionic exclusion processes, while others conduct electrically but have a capillary pressure too great for hydraulic flow. The efficacy of the hydraulic model over the electrical model for carbonates might indicate that electrical transport in carbonates and particularly in tight carbonates is more effective than hydraulic transport and consequently the electrical model underestimates the permeability in such rocks.

Consequently, there are at least three possible models for calculating the permeability using the Katz and Thompson approach (Katz and Thompson, 1986; 1987; Thompson *et al.*, 1987). The first is using the critical characteristic length L_c , where

$$k_{LHc} = C_1 L_c^2 G = \frac{C_1 L_c^2}{F}, \quad (S1)$$

where the constant $C_1 = 1013/226$. The parameter G is the connectedness (Glover, 2009; 2010), which is the ratio of the conductivity of the rock fully saturated with a conducting fluid to the conductivity of that fluid and is the inverse of the formation factor defined by

Archie (1942). Consequently, $G = \sigma_0 / \sigma_w = \phi^m$, where m is the cementation exponent. The cementation exponent in reservoir rocks can vary from about 1 for fractured rocks to over 4 for some carbonates and should always be measured rather than assumed because its presence as an exponent makes the connectedness and formation factor extremely sensitive to its value (Glover, 2015). It is worth noting that the dimensionality $[L]^2$ of permeability is accounted for entirely by the length squared term in Eq. (S1) because all other terms are dimensionless.

Katz and Thompson showed that it was possible to obtain the conductivity ratio from a combination of L_c , L_{Emax} and S_{LEmax} which is the fraction of connected pore volume filled with mercury at L_{Emax} according to $G = \sigma_0 / \sigma_w = L_{Emax} \phi S_{LEmax} / L_c$, allowing a new model for permeability to be written

$$k_{LE} = C_1 L_c L_{Emax} \phi S_{LEmax} \quad (S2)$$

where the term $L_c L_{Emax}$ provides the length-squared dimensions required for permeability and the term ϕS_{LEmax} represents the fraction of the whole rock filled with mercury at L_{Emax} . This is the Katz and Thompson electrical model.

Katz and Thompson also introduced a third model based on the hydraulic length scale L_{Hmax}

$$k_{LH} = C_2 \left(\frac{L_{Hmax}^3}{L_c} \right) \phi S_{LHmax} \quad (S3)$$

where the term L_{Hmax}^3 / L_c provides the length-squared dimensions required for permeability, S_{LHmax} is the fraction of connected pore volume filled with mercury at L_{Hmax} , and the term ϕS_{LHmax} represents the fraction of the whole rock filled with mercury at L_{Hmax} . In this case the constant $C_2 = 1013/89$. It is this last model that performs best in carbonates and that is included in the main paper.

Comisky *et al.* (2007) have noted that all of the Katz and Thompson models are analytically derived and do not depend upon calibration to a given dataset even though Katz and Thompson did compare their models to experimentally derived data over the range 5 μ D to 5 D with some success.

Berg Fontainebleau Sandstone Model

Berg implemented a version of their model as an empirical fit valid for Fontainebleau sandstone (Berg, 2014). While it was not expected that this version of the model would

perform well for tight carbonates, and indeed does not, we have implemented this model under the name ‘Berg Fontainebleau model’. It is given by

$$k_{BERGFont} = 1329(\phi - 0.054)^{2.12}(\phi - 0.030). \quad (\text{S4})$$

Poiseuille-based models

Swanson Model

Swanson (Swanson, 1981) proposed a permeability model where the permeability is controlled by a single point on the capillary pressure curve that is characterised by the apex of the plot of mercury saturation as a function of mercury saturation S_b , and which shares a great similarity to the equation of Thomeer (1960). The general formula used by Swanson is given by

$$k = C_3 \left(\frac{S_b}{P_c} \right)_{Apex}^{a_1}, \quad (\text{S5})$$

where C_3 and a_1 are empirically-determined constants. Swanson determined the constants by calibrating Eq. (S4) with data from 319 gas measurements on sandstone and carbonate rocks (203 clastic samples from 41 formations, and 116 carbonate samples from 330 formations) with a range of permeabilities from 20 μD to 2 D, and which were not Klinkenberg corrected, to obtain $C_3 = 399$ and $a_1 = 1.691$. It was recognised that such a correlation would be dependent on the sample set and that it would be particularly prone to error in tight rocks where slippage effects are more prevalent. Consequently, Swanson (1981) carried out a smaller calibration using 24 clean samples of sandstone upon which steady-state brine permeability was measured under a net stress of 1000 psi, to obtain $C_3 = 431$ and $a_1 = 2.109$.

It should be noted that the general equation used by Swanson (1981) (Eq. (S5)) is formally the same as the Katz and Thompson (Katz and Thompson, 1986; 1987; Thompson *et al.*, 1987) electrical length scale model (Eq. (S2)), but gives different values of permeability when implemented because the Swanson version depends upon the Swanson calibrations.

Wells-Amaefule Model

The method of predicting permeability from capillary pressure proposed by Wells and Amaefule (1985) represents a modification and extension to the approach of Swanson (1985)

with technical improvements to the approach for determining the apex value and a calibration to tight sandstones. Wells and Amaefule (1985) calibrated the general Swanson equation with 35 samples of tight sandstone from two formations that varied between 20 nD and 70 mD, making their measurements under pressures between 3000 and 4000 psi using a gas pulse decay method with corrections for slippage and net overburden effects, obtaining the parameters in Eq. (S5) as $C_3 = 30.5$ and $a_1 = 1.56$. The Wells-Amaefule is best regarded as the same as the Swanson model but with some technical modifications and a different calibration designed to perform better in tight gas sands.

Kamath 'Model'

More recently Kamath (1992) has aggregated data from a number of different datasets including those of Katz and Thompson (1986), Swanson (1985) and Wells and Amaefule (1985) as well as some newly measured values to provide a new dataset for calibrating permeability models. The new dataset had 454 samples covering a very large range from 20 nD to 2 D. Despite the very large range of the measurements, their varied measurement methods; some being steady-state gas, some steady-state brine, some pulse-decay, and the awkwardness of some being corrected for slippage and net overburden while others were not, Kamath (1992) propose their model as valid for tight gas sands. After calibration with the dataset the Kamath model is given by Eq. (S5) with $C_3 = 413$ and $a_1 = 1.85$. The Kamath 'model' is, in fact, a misnomer. It is simply the Swanson model but calibrated with a larger dataset that is not self-consistent.

Dastidar *et al.* Model

Dastidar *et al.* (2007), have provided a model that looks very similar to that of Winland and is given by

$$k_{Dastidar} = C_6 R_{wgm}^{a_6} \phi^{a_7} . \quad (S6)$$

The main difference is in the value of R_{wgm} . Dastidar *et al.*, (2007) followed the approach of Glover *et al.* (2006a; 2006b; 2006c) in calculating the characteristic length scale from the weighted geometric mean of a length scale distribution. In the case of Glover *et al.* (2006a; 2006b; 2006c) it was the weighted geometric mean of the grain diameter that was used in the RGPZ model. Dastidar *et al.*, (2007) calculated the weighted geometric mean of the pore size from MICP data. In both cases, the weighted geometric mean describes the mixing of

randomly arranged arbitrary shaped sub-volumes of the rock, each characterised by a single size on the respective distribution, and each of a volume given by the weighting. The weighted geometric mean is best computed in logarithmic space in order to avoid runaway inflation of the product, and is given by

$$\ln\langle x \rangle_g = \frac{\sum_{i=1}^N w_i \ln x_i}{\sum_{i=1}^N w_i} , \quad (\text{S7})$$

where $\langle x \rangle_g$ is the weighted geometric mean value of a distribution of N values of x_i each with weighting w_i . In the case of Dastidar *et al.* (2007) it is the pore radius distribution that is being considered and the weighted geometric mean is R_{wgm} . In the case of Glover *et al.* (2006a; 2006b; 2006c) the distribution being considered is the grain diameter.

The big difference between the Dastidar *et al.* (2007) model and the geometric mean implementations of the RGPZ model is that the RGPZ model requires no empirical calibration, being derived analytically, while that of Dastidar *et al.* requires three empirical constants which were obtained by calibration with unsteady-state Klinkenberg-corrected gas permeability measurements on 150 samples with permeabilities ranging from microdarcies to darcies and porosities ranging from 0.01 to 0.30. They obtained $C_6 = 4073$, $a_6 = 1.64$, and $a_7 = 3.06$.

Huet *et al.* Model

Dastidar *et al.* (2007) and some implementations of the RGPZ model (Glover *et al.*, 2006b; 2006c) attempted to account for the full range of grain sizes in the permeability prediction. Huet *et al.* (2005) approached the same problem but from the point of view of the capillary pressure. Their approach is to relate the predicted permeability to a fit to the whole capillary pressure curve using the Brooks-Corey methodology. The consequence is a permeability prediction equation that requires knowledge of the displacement pressure P_d , Brooks-Corey parameter λ and the irreducible water saturation S_{wi} as well as the porosity ϕ , together with five empirically determined coefficients. The coefficients were found by calibrating the model against a dataset containing 89 sandstone samples which spanned a wide range of permeability (4.1 μD – 8340 mD) and porosity (0.003 – 0.34). Their measurements were made at 800 psi net confining pressure using a steady-state method and were Klinkenberg corrected. The large number of fitting parameters ensured that a good fit was possible to the calibrating dataset, but makes the method more sensitive to errors arising from its use with

other rocks than some of the other models tested in this paper. The calibration with 89 data points probably does not justify the quotation of the coefficients to between 5 and 9 significant figures. The Huet *et al.* (2005) model is given by

$$k_{HB} = C_6 \frac{1}{P_d^{a_6}} \left(\frac{\lambda}{\lambda+2} \right)^{a_7} (100 - S_{wi})^{a_8} \phi^{a_9} \quad , \quad (\text{S8})$$

where, $C_6 = 81718.8669$, $a_6 = 1.7846$, $a_7 = 1.6575$, $a_8 = 0.5475$, and $a_9 = 1.6498$, with P_d in psi and S_{wi} in percent.

PERMEABILITY MODEL ASSESSMENT

Figure S1 shows the performance of the eight models that were judged too ineffective to be used for permeability prediction in carbonate samples together with a 1:1 line indicating a perfect prediction as well as high and low bounds representing a variance of ± 2.5 (i.e., upper and lower bounds representing 2.5 times greater or less than a perfect prediction, respectively). A simple judgement concerning the goodness of prediction is that the prediction falls between the variance ± 2.5 limits.

It is immediately clear that the permeabilities predicted by this set of models range over five orders of magnitude, commonly predicting permeabilities that are hundreds of times too large or too small.

Figure S1 shows that both the Katz and Thompson critical length and electrical length model provide good permeability predictions for about half of the samples, but badly underestimate the other half, with some predictions being up to 2 orders of magnitude too small.

As we predicted above, the failure of the electrical length model occurs because the electrical connectivity of the rock differs significantly from the hydraulic connectivity. Although both hydraulic and electrical flow in tight carbonates are confined to extremely thin intercrystalline pathways, narrow pore throats that are electrically open are not necessarily hydraulically patent due to the high capillary pressures that need to be overcome for flow to occur.

The Berg (2014) implementation for Fontainebleau sandstone did not predict the permeabilities of our tight carbonate samples well as expected, and should not be taken to indicate the quality of this method in general. However, our implementation of the generic

form of the Berg (2014) equation (Eq. (7) in the main paper) using the constriction factor C_s as an adjustable parameter provided good permeability predictions.

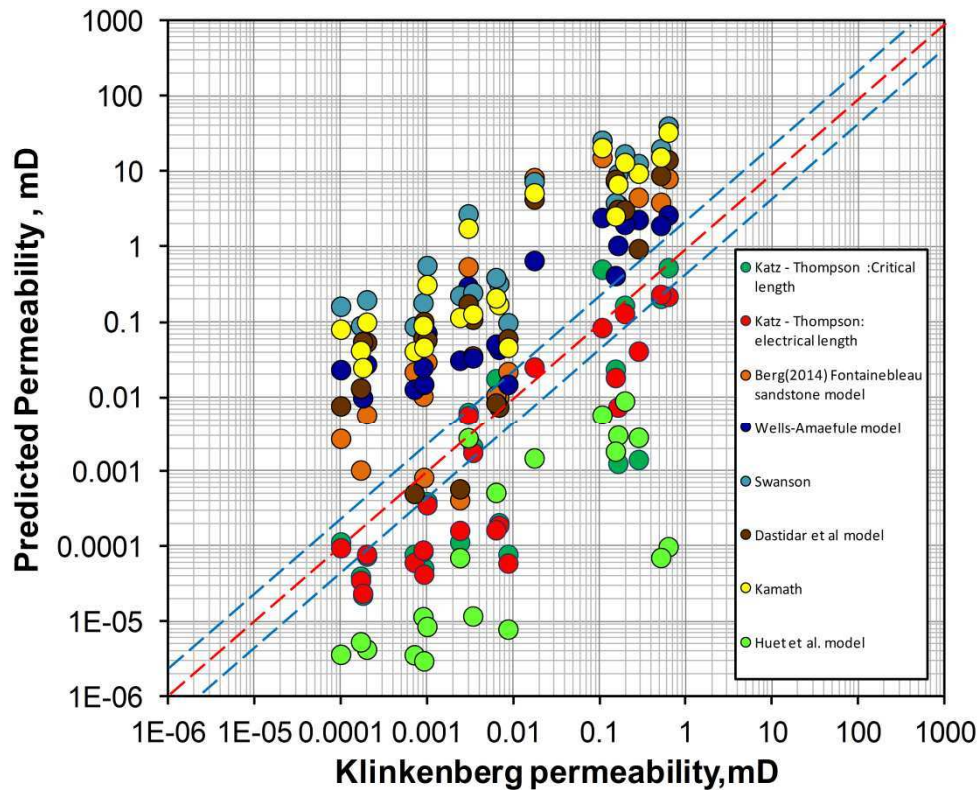


Figure S1. Predicted permeabilities as a function of measured permeabilities for the poorly calibrated models, together with a 1:1 perfect agreement and variance lines set at ± 2.5 . For (Huet et al model) $\lambda=0.2$ and $S_{wi}=0.2$.

The Poiseuille-based models generally performed badly despite the large number of parameters and coefficients they often use with exception of the Winland and Pittman models (Kolodzie, 1980; Comisky et al., 2007; Gunter et al., 2014). These models commonly overestimated the permeability by between two and three orders of magnitude. Perhaps the worst performance of all of the models was that of Swanson (1981), which provided overestimates of the permeability by between 2 and 3 orders of magnitude, and which saw only one of the samples falling within the ± 2.5 variance limits.

The Wells-Amaefule model (Wells and Amaefule, 1985) is derived from the Swanson method and would be expected to perform similarly. Wells-Amaefule model does indeed produce predictions which are similar to those of Swanson, but with a degree of overestimation reduced to between one and two orders of magnitude. This, however, is still a

very significant error, and there was only one sample for which the Wells-Amaefule model produced a prediction within the ± 2.5 variance criterion.

The Kamath 'model' (Kamath, 1992) uses the same apex point as the Swanson model differing only in the dataset that it used to calibrate the model. As expected, this model also fails badly, performing very similarly to the Swanson model.

The Dastidar *et al.* (2007) model, as we have seen, is very similar to that of Winland model (Kolodzie, 1980; Comisky *et al.*, 2007; Gunter *et al.*, 2014) that performs well and is discussed in the main paper, differing only in the weighted geometric mean that is used to calculate the effective radius. One might, therefore, expect this model to produce similarly good results. However, the Dastidar *et al.* (2007) model did not perform well, over-estimating permeability by as much as two orders of magnitude for most of the samples tested, and obtaining a prediction within the ± 2.5 variance limits for only 18% of the samples. The reason for the difference between the Dastidar *et al.* (2007) and the Winland (Kolodzie, 1980; Comisky *et al.*, 2007; Gunter *et al.*, 2014) model may be important as it implies that not all of the pore size distribution contributes to the overall permeability of the rock. That in itself is not a revolutionary idea; after all the contribution to permeability made by very small pores will be rather small as result of the operation of capillary pressures and the Poiseuille equation, while the contribution to permeability made by very large pores might be rather small if the only way to flow fluid between them is so much smaller pores as was found in the carbonates with moldic porosity by Rashid *et al.* (2015). The conclusion is that the permeability will be overestimated if we incorporate permeability contributions from the very large pore sizes as well as the very small pore sizes, as occurs in the Dastidar *et al.* (2007) approach, and that a well-chosen characteristic pore radius would be more appropriate.

One of the worst predictions obtained in this study was from the use of the Huet *et al.* (2005) model. Although this is a complex model, it consistently provided predictions that fell outside the ± 2.5 variance limits for all but one sample, often underestimating the permeability by 3 to 4 orders of magnitude. Variation of the lambda and irreducible water saturation has little effect on the resulting permeabilities which are strongly controlled by the displacement pressure. Displacement pressures are very high in these tight carbonates and consequently the predicted permeabilities are very low; much lower than the measured values. The Huet *et al.* (2005) model takes the entire capillary pressure curve into account when predicting the permeability. Unfortunately, entire capillary pressure curves are not available from downhole

measurements, so the model would be of limited practical utility even if it provided accurate permeability predictions in tight carbonates.

Ironically perhaps, the Huet *et al.* (2005) model uses as many as four variable parameters and five empirically determined coefficients. A model with a large number of adjustable parameters should be capable of producing more accurate predictions. It is instructive to note that with the exception of the Huet *et al.* (2005) model, those models which perform best in the prediction of permeability in carbonate rocks are the simplest. The Generic and RGPZ models require either no or one empirical coefficient depending on how they are used and account for 3 of the best 5 models.

CONCLUSIONS

In conclusion, all of the models described in this supplementary material do not perform well in the carbonate rocks we tested. That does not mean that they are bad models and each could perform very well in other facies types. Often, analysis of the reasons for their failure are as instructive as the reasons why other models perform well.

REFERENCES

- ARCHIE, G.E. 1942. The electrical resistivity log as an aid in determining some reservoir characteristics: Transactions of the American Institute of Mechanical Engineers, 146, 54–67.
- BERG, C.F. 2014. Permeability Description by Characteristic Length, Tortuosity, Constriction and Porosity. *Transport in Porous Media*, 103(3), pp. 381-400.
- COMISKY, J.T., NEWSHAM, K., RUSHING, J.A. & BLASINGAME, T.A. 2007. A Comparative Study of Capillary-Pressure-Based Empirical Models for Estimating Absolute Permeability in Tight Gas Sands. Society of Petroleum Engineers.
- DASTIDAR, R., SONDERGELD, C.H. & RAI, C.S. 2007. An Improved Empirical Permeability Estimator From Mercury Injection For Tight Clastic Rocks.
- GLOVER, P.W.J. 2009. What is the cementation exponent? A new interpretation. *Leading Edge* (Tulsa, OK), 28(1), pp. 82-85.
- GLOVER, P.W.J. 2010. A generalized Archie's law for n phases. *Geophysics*, 75(6), pp. E247-E265.
- GLOVER, P.W.J. 2015. Geophysical Properties of the Near Surface Earth: Electrical Properties. In: Gerald Schubert (editor-in-chief) *Treatise on Geophysics*, 2nd edition, Vol 11. Oxford: Elsevier; 2015. p. 89-137.
- GLOVER, P.W.J., ZADJALI, I.I. & FREW, K.A. 2006a. Permeability prediction from MICP and NMR data using an electrokinetic approach. *Geophysics*, 71(4), pp. F49-F60.

- GLOVER, P.W.J., ZADJALI, I. & FREW, K. 2006b. Permeability prediction from MICP and NMR data using an electro-kinetic approach, Poster, EGU 2006, EGU06-A-01566, Vienna, 2-7 April 2006.
- GLOVER, P.W.J., ZADJALI, I. & FREW, K. 2006c. A new equation for permeability prediction derived from electro-kinetic theory., Oral, GAC-MAC-SEG-SGA 2006, Abstract No. 758, Montréal, 14-17 May 2006.
- GUNTER, G.W., SPAIN, D.R., VIRO, E.J., THOMAS, J.B., POTTER, G., & WILLIAMS, J. 2014. Winland Pore Throat Prediction Method - A Proper Retrospect: New Examples From Carbonates and Complex Systems. Society of Petrophysicists and Well-Log Analysts SPWLA-2014-KKK, SPWLA 55th Annual Logging Symposium, 18-22 May, Abu Dhabi, United Arab Emirates.
- HUET, C.C., RUSHING, J.A., NEWSHAM, K.E. & BLASINGAME, T.A. 2005. A Modified Purcell/Burdine Model for Estimating Absolute Permeability from Mercury-Injection Capillary Pressure Data. International Petroleum Technology Conference, Doha, Qatar, Nov. 21-23, Paper IPTC 10994.
- KAMATH, J. 1992. Evaluation of Accuracy of Estimating Air Permeability From Mercury-Injection Data.
- KATZ, A.J. & THOMPSON, A.H. 1986. Quantitative prediction of permeability in porous rock. *Physical Review B*, 34, 8179-8181.
- KATZ, A.J. & THOMPSON, A.H. 1987a. Prediction of rock electrical conductivity from mercury injection measurements. *Journal of Geophysical Research: Solid Earth*, 92, 599-607.
- KOLODZIE, S., JR. 1980. Analysis Of Pore Throat Size And Use Of The Waxman-Smits Equation To Determine Ooip In Spindle Field, Colorado. Society of Petroleum Engineers.
- RASHID, F., GLOVER, P.W.J., LORINCZI, P., COLLIER, R., & LAWRENCE, J. 2015. Porosity and permeability of tight carbonate reservoir rocks in the north of Iraq, *Journal of Petroleum Science and Engineering*, 133, 147-161, <http://dx.doi.org/10.1016/j.petrol.2015.05.009>
- SWANSON, B. F. 1981. A Simple Correlation Between Permeabilities and Mercury Capillary Pressures.
- THOMEER, J.H.M. 1960. Introduction of a pore geometrical factor defined by the capillary pressure curve. *Pet. Tech*, 73-77.
- THOMPSON, A.H., KATZ, A.J., & RASCHKE, R.A. 1987. Estimation of Absolute Permeability from Capillary Pressure Measurements. Paper SPE 16794 presented at the 1987 SPE Annual Technical Conference and Exhibition, Dallas, TX, Sept. 27-30.
- WELLS, J.D. & AMAEFULE, J.O. 1985. Capillary Pressure and Permeability Relationships in Tight Gas Sands. Society of Petroleum Engineers.